Ecological Indicators 180 (2025) 114371

Contents lists available at ScienceDirect

Ecological Indicators

journal homepage: www.elsevier.com/locate/ecolind

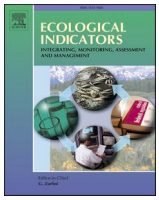

Original Articles

Potential use of multi-year UAV imagery for monitoring vegetation traits in grasslands

Batnyambuu Dashpurev [a,*], David R. Piatka [a], Alexander Krämer [b], Anne Schucknecht [c], Klaus Butterbach-Bahl [a,d], Ralf Kiese [a]

[a] Institute of Meteorology and Climate Research, Atmospheric Environmental Research (IMK-IFU), Karlsruhe Institute of Technology (KIT), Kreuzeckbahnstr. 19, 82467 Garmisch-Partenkirchen, Germany
[b] WWL Umweltplanung und Geoinformatik GbR, Mozartweg 8, 79189 Bad Krozingen, Germany
[c] Earth Observation Applications Team, OHB System AG, Manfred-Fuchs-Str. 1, 82234 Weßling - Oberpfaffenhofen, Germany
[d] Pioneer Center Land-CRAFT, Department of Agroecology, University of Aarhus, Ole Worms Allé 3, Bld. 1171, 8000 Aarhus, Denmark

ARTICLE INFO

Keywords:
Unmanned aerial vehicle
Machine learning
Aboveground biomass
Vegetation carbon
Vegetation nitrogen
Carbon to nitrogen ratio
Plant species richness
Shannon H-index

ABSTRACT

Permanent grasslands in Germany are characterized by the intensity of management practices. The intensity of management significantly influences both the biodiversity and ecosystem services provided by grasslands. Therefore, monitoring vegetation traits of intensively managed grasslands is crucial for making management decisions aimed at maximizing ecosystem services and minimizing environmental footprints of grassland cultivation. In intensively managed grasslands, aboveground dry biomass (AGB_{dry}), plant species richness, vegetation carbon (C) and nitrogen (N) content, and carbon to nitrogen (C:N) ratio serve as key indicators to assess the condition of the grassland, an information which is highly relevant for farmers, inspectors, and decision-makers. This study aimed to accurately estimate AGB_{dry}, N, C:N ratio, plant species richness, and Shannon H-index in two study areas in Bavaria, Germany using multi-year *in-situ* measurements and corresponding unmanned aerial vehicle (UAV) imagery. The combined *in situ* and UAV dataset was collected at different grassland sites (Fendt, Rottenbuch, and Bayreuth area) between 2019 and 2023, partly at several times during one year. Therefore, the dataset covers both intra- and inter-annual growth patterns (April to October). UAV images were radiometrically calibrated using a reflectance target and processed with Pix4D's internal radiometric corrections. Both Random Forest and Extreme Gradient Boosting (XGBoost) were used to estimate grassland traits. The regression models were trained using the *in-situ* measurements, and as predictor variables the corresponding reflectance in the spectral bands of the multispectral UAV imagery and the derived vegetation indices. Model performance was assessed using an independent validation dataset, consisting of 20 % of the reference data that were not included in the model training stage. To improve estimation accuracy, we conducted test cases by training the regression models using different training data subsets. As a result, we derived multi-year vegetation trait maps from UAV imagery with R^2 values of 0.81 for AGB_{dry}, 0.77 for N content, 0.81 for the C:N ratio, 0.84 for SR and 0.86 for H-index, respectively. Overall, the study highlights the potential of integrating multi-year *in situ* data with UAV imagery to create multidimensional datasets that effectively capture spatial and temporal changes in vegetation traits.

1. Introduction

Permanent grasslands cover about one-third of Germany's agricultural land area and are particularly valuable as they provide a wide range of ecosystem services (Kirschke et al., 2021). For instance, these services range from provisioning (e.g., food production), regulating (e.g., climate regulation) to supporting (e.g. biodiversity) as well as cultural aspects (e.g., recreational activities) (Bengtsson et al., 2019; Zhao et al., 2020). Among these, one of the most important economic ecosystem services provided by grasslands is the provision of food for dairy and cattle farming (Schoof et al., 2020). Therefore, permanent grassland in Germany is primarily used to produce fodder through regular mowing and grazing. From a climate change mitigation perspective, grasslands have long been recognized for their significant

* Corresponding author.
E-mail address: batnyambuu.dashpurev@kit.edu (B. Dashpurev).

https://doi.org/10.1016/j.ecolind.2025.114371
Received 16 May 2025; Received in revised form 24 September 2025; Accepted 27 October 2025
Available online 4 November 2025

role in carbon storage and sequestration, and their high species richness, which enhances their resilience to altered precipitation patterns and increasing temperatures (Feigenwinter et al., 2023; Gomez-Casanovas et al., 2021; Korell et al., 2024). On the other hand, ongoing climate change is significantly affecting grasslands (Bardgett et al., 2021), especially in intensively managed areas, where both biomass productivity and fodder quality are increasingly impacted by changing climate conditions (Berauer et al., 2020; Dumont et al., 2015; Korell et al., 2024; Li et al., 2018). Therefore, spatially explicit information on vegetation traits is crucial for developing adaptation strategies and sustaining productivity and ecosystem functions in managed grasslands under a changing climate.

Agriculturally used grasslands are found across all regions of Germany although the intensity of management varies. In the (pre-)Alpine regions, there are widespread grassland landscapes that are not only used for livestock fodder but also serve as important recreational areas (Schmitt et al., 2024; Schwarz et al., 2018). (Pre-)Alpine grasslands are characterized by their unique biodiversity and species richness and have historically been used as a source of fodder for livestock for centuries (Fumy et al., 2023; Kiese et al., 2018; UNESCO World Heritage Centre, 2015). Grassland management in this region includes both extensive and intensive approaches, with higher grazing pressure, and more frequent fertilizer application and mowing frequency in intensively managed areas (Vogt et al., 2019). To increase the economic efficiency of grasslands, farmers often aim to achieve higher biomass productivity rates, which typically puts a lot of pressure on biodiversity, resulting in reduced species richness (Fumy et al., 2023; Mayel et al., 2021). Furthermore, intensive grassland management may lead to various negative environmental impacts, e.g., water pollution (Bobbink et al., 2022; Schlingmann et al., 2020), soil degradation (Seeger, 2023), and increased greenhouse gas emissions (Hörtnagl et al., 2018; Offermanns et al., 2023). In particular, the management intensity can significantly influence the ecosystem quality and health of grasslands, as indicated by botanical composition, by altering plant diversity (Gilhaus et al., 2017). Therefore, there is a high demand for accurate estimation of vegetation traits at local to landscape scales, providing valuable information for both farmers and decision-makers.

Over the past decade, UAVs have developed rapidly and are increasingly being used in the agricultural sector, with UAVs differing in design, range, and installed sensors depending on their intended use. Many types of sensors (e.g., multispectral, hyperspectral, thermal, and Light Detection and Ranging (LiDAR)) are continuously being developed and made available for the agricultural sector, especially for monitoring of grasslands and croplands (Norasma et al., 2019; Raj et al., 2019; Zhang et al., 2024). However, UAV-based methods are costly and time-consuming for large areas, especially when equipped with a wide range of spectral bands (e.g., hyperspectral sensors); therefore, multispectral sensors (visible/near-infrared) are predominantly used (Zhang et al., 2024). Most popular bands in multispectral sensors include red (620–750 nm), green (495–570 nm), near-infrared (NIR, 780–1000 nm), and red-edge (RE, 680–730 nm). Among them, NIR and red-edge bands are particularly effective for vegetation trait estimation, as NIR is sensitive to leaf structure and biomass, while the red-edge band responds strongly to chlorophyll and nitrogen content, making them valuable for estimating N, C:N ratio, and biomass (Arogoundade et al., 2023; Bazzo et al., 2023a). For example, recent studies by Biswal et al. (2024), Furnitto et al. (2025), and Gao et al. (2025) demonstrated that NIR and red-edge bands are particularly useful for analyzing vegetation traits. Vegetation indices derived from combinations of visible bands and NIR have already proven to be a useful method for assessing a wide range of vegetation traits (Huang et al., 2021; Thornley et al., 2023; Zhang et al., 2024). For instance, the Normalized Difference Vegetation Index (NDVI), Soil-Adjusted Vegetation Index (SAVI), and Perpendicular Vegetation Index (PVI) are the most effective and frequently used indices for estimating various vegetation traits because they strongly correlate with biophysical variables such as biomass, canopy cover, and height, and leaf chlorophyll content (Raj et al., 2019; Verrelst et al., 2019; Vidican et al., 2023; Xue & Su, 2017). However, these indices often show weak relationships with plant biogeochemical properties (Arogoundade et al., 2023). As an alternative, the red edge band and its derived indices are sensitive to biogeochemical variables and are frequently used for estimating vegetation N and C:N ratios (Arogoundade et al., 2023; Zhang et al., 2024). For example, recent studies have clearly demonstrated that the Red Edge Normalized Difference Vegetation Index ($NDVI_{red\text{-}edge}$) and Red Edge Simple Ratio ($SR_{red\text{-}edge}$) have the potential to estimate the plant N content and C:N ratios (Berger et al., 2020; Bronson et al., 2020; Walsh et al., 2018; Zhang et al., 2024). Therefore, the vegetation traits could be estimated with reasonable accuracy by combining the aforementioned spectral bands and indices in machine learning (ML).

ML techniques are becoming an important tool for estimating various vegetation characteristics from remotely sensed data by training them on field reference measurements (Janga et al., 2023). Such methods combine statistical modeling and complex algorithms to perform various prediction tasks with relatively high accuracy. In recent times, there have been numerous efforts in estimating vegetation traits using various ML algorithms, including aboveground biomass (Morais et al., 2021; Wang et al., 2022), plant species diversity (Fauvel et al., 2020; Zhao et al., 2022), plant N and C content (Ennaji et al., 2023; Peerbhay et al., 2022), as well as C:N ratio (Arogoundade et al., 2023; Gao et al., 2020). In particular, classic ML algorithms such as Random Forest (RF), Decision Trees (DT), Logistic Regression (LR), and Gradient Boosting Machines (GBM) are widely employed in estimating various vegetation traits due to their robustness and flexibility in handling complex relationships of remote sensing and *in-situ* data in reasonable accuracy (Ennaji et al., 2023; Janga et al., 2023). Specifically, ML models developed using RF and GBM perform well and have achieved promising results for biomass estimation; however, predicting N content proved to be challenging due to limited spectral features and availability of training data (Schucknecht et al., 2022). Particularly, automated ML (AutoML) has more recently emerged as an accessible and efficient technique (He et al., 2021). AutoML uses an ensemble learning approach that combines multiple algorithms or statistical models into a stronger model to improve overall prediction so that this technique can provide an efficient evaluation of numerous ML algorithms (Salehin et al., 2024). However, ML algorithms typically require large amounts of high-quality training data, and when datasets are limited, the models can overfit (Janga et al., 2023). Their performance also depends on how well the training samples represent different sites and conditions, which may limit generalizability. For example, recent studies have shown that models trained in one region often lose accuracy when applied to different regions without re-calibration (Lemenkova, 2025; Morais et al., 2021). Furthermore, Kupidura et al. (2024) reported that ML performance is highly sensitive to the size of the training sample. Therefore, ML performance could be improved by increasing the size and diversity of the training dataset, for example, using multi-year datasets of *in situ* and associated remote sensing data.

The major aim of the present study is to provide a UAV imagery-based key vegetation traits monitoring product that can support grassland management and further socio-economic modeling in the (pre-) Alpine grasslands. In this respect, this study aimed to estimate key vegetation traits by combining multi-year datasets of *in situ* and associated UAV imagery using different ML regression models and assessing the spatiotemporal patterns of vegetation traits. First, we derived key vegetation traits, including AGB_{dry}, vegetation N content, C:N ratio, species richness, and Shannon H-index, in two study areas. Second, we conducted a spatiotemporal analysis to assess intra- and inter-annual changes in vegetation traits across several selected grassland sites, and third, we evaluated the predictive power and the potential of using multi-year data to predict vegetation traits at different locations and times.

2. Data and methods

2.1. Study area

The study was conducted at five sites of permanent grassland in Bavaria, Germany (Fig. 1a-f). The study sites of Rottenbuch (769 m above sea level (a.s.l.;) Fig. 1b) and Fendt (595 m a.s.l.; Fig. 1c) are located in southern Bavaria and are part of the TERENO Pre-Alpine Observatory (Kiese et al., 2018). The study sites in northern Bavaria around Bayreuth (340 m a.s.l.) include Gubitzmoos (Fig. 1d), Schobertsberg (Fig. 1e), and Obernschreez (Fig. 1f).

The Fendt and Rottenbuch sites are characterized by a hilly, prealpine landscape. This region is characterized by a humid continental climate with an average annual precipitation of 956–1109 mm and an average annual temperature of 8.8–8.9 °C. The vegetation cover in these grasslands is primarily dominated by meadow grasses such as *Festuca rubra* L., *Poa pratensis* L., and *Lolium perenne* L., along with a variety of herbs and legumes, including *Ranunculus repens* L., *Trifolium pratense* L., and *Trifolium repens* L (Stadler et al., 2017; Kiese et al., 2018).

The study sites around Bayreuth are located in the part of the western foothills of the Franconian Switzerland, which is characterized by mid-altitude mountain ranges. The study region has a humid continental climate, with a mean annual precipitation of 724 mm and a mean annual temperature of 8.3 °C. The potential dominant vegetation cover in the grassland around Bayreuth included *Taraxacum* sect. *Ruderalia*, *Dactylis glomerata*, *Plantago lanceolata*, *Trifolium pratense* L., *Ranunculus acris* L., *Holcus lanatus*, and *Elymus repens* (L.) Gould (Maria Dittmann, 2018; Schmitt et al., 2022).

Grasslands in both regions have a long history of frequent mowing, grazing, and regular fertilization for fodder production. Grassland management practices at the study sites vary from extensive management (1–2 mowings per year with no fertilizer application) to intensive management (4–6 mowings per year with 4–5 slurry applications) (Petersen et al., 2021; Schmitt et al., 2022; Schucknecht et al., 2020).

2.2. Datasets

2.2.1. UAV image collection

Multi-year UAV imagery was collected between May 2019 and July 2023 using a fixed-wing UAV (eBee, senseFly, Cheseaux-sur-Lausanne, Switzerland). The fixed-wing UAV was equipped with a four-band Parrot Sequoia sensor (SEQ; Parrot Drones SAS, Paris, France), which was used to acquire green (G), red (R), RE, and NIR multispectral imagery. In addition, the UAV was equipped with irradiance sensors ("sunshine sensors") mounted on top to measure the incoming solar radiation. The UAV images were acquired at a flight altitude of 85 m, with a ground

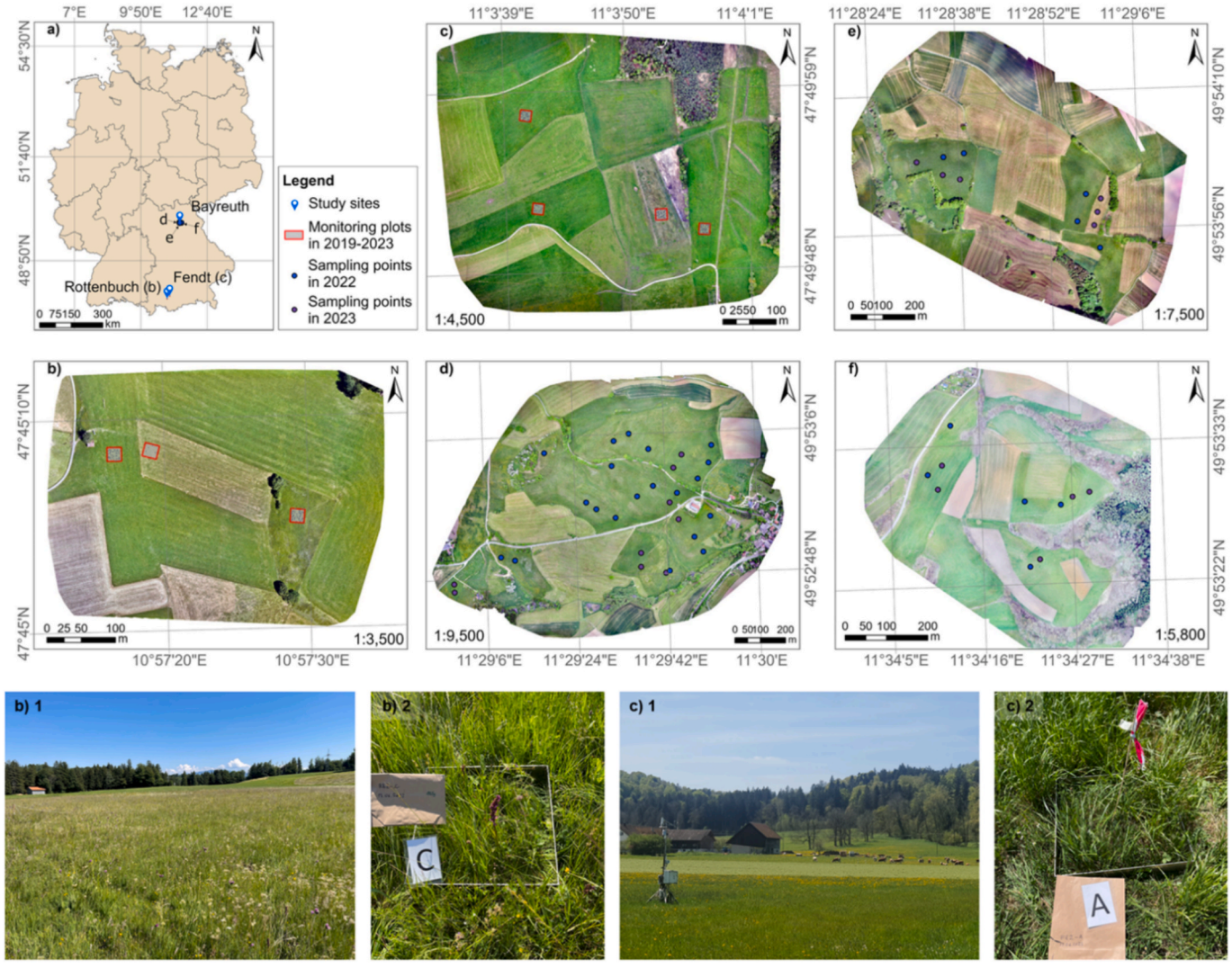

Fig. 1. Location of study site: Overview of the sites within Germany (a). Aerial view of the monitoring plots in Rottenbuch (b) and in Fendt (c). Here, the images below show one of sampling plots in Rottenbuch (b1–b2) and Fendt (c) 1–c2). Sampling plots in Bayreuth: Gubitzmoos (d), Schobertsberg (e) and Obernschreez (f).

resolution of approximately 8 cm/pixel. Both lateral and longitudinal overlaps were maintained at 80 % to ensure sufficient coverage and image quality. A detailed description of the sensor and the processing of the UAV images can be found in Schucknecht et al. (2022).

The processing of the UAV images was done with the Pix4dMapper Pro software (Pix4D S.A., Prilly, Switzerland) and consisted of three steps. The photogrammetric processing was based on a structure from motion (SfM) approach (Kameyama & Sugiura, 2021). First, key points of the images were extracted and matched, and the internal (e.g. focal length) and external (e.g. orientation) parameters of the camera were calibrated. The georeferencing was done by integrating measured ground control points (GCPs) and identifying them on several input images. Coordinates of GCPs were measured with the Trimble DGPS. As a result, georeferenced automated control points were created. The second step was to densify the point cloud according to the pix4D standard template for agricultural applications. The final step was to mosaic the adjusted and calibrated individual images into orthophotos and final reflectance images. The reflectance targets were used to perform an additional radiometric calibration with respect to field conditions, taking into account the illumination conditions at the date, time and location of the image acquisition, as well as some sensor characteristics. This provides absolute reflectance values that can be compared between different cameras or flights.

After image processing, a set of spectral vegetation indices was calculated from the different reflectance bands for each image acquired. The spectral vegetation indices were selected based on how they contributed to the estimation of vegetation traits in previous studies (Schucknecht et al., 2022; Dashpurev et al., 2023) and a recent comprehensive literature review (Zhang et al., 2024). Consequently, we selected seven indices to be used as additional predictors for the estimation of vegetation traits. These indices are the NDVI, $NDVI_{red\text{-}edge}$, $NDVI_{green}$, SAVI, Modified Soil Adjusted Vegetation Index (MSAVI), Transformed Soil Adjusted Vegetation Index (TSAVI) and Red-Edge Simple Ratio ($SR_{red\text{-}edge}$) (Montero et al., 2023). Finally, a multidimensional dataset was created by combining the time series of reflectance images and spectral vegetation indices using the multidimensional toolbox in ArcGIS Pro 3.2.

2.2.2. *In-situ field data*

Field campaigns were conducted along with UAV imaging to collect intra- and inter-annual *in situ* vegetation data at the Fendt, Rottenbuch, and Bayreuth field sites between 2019 and 2023 (Table 1). At each site, a 20 m × 20 m plot was sampled in four 0.5 m × 0.5 m subplots after UAV imaging. In each subplot, the bulk canopy height was measured with a plate meter. The vegetation was cut at 7 cm above the soil surface to obtain the fresh weight. A Trimble DGPS with centimeter-level accuracy was used to determine the location of each plot. In the laboratory, the dry weight of the samples was determined after drying the samples in an oven at 65 °C until constant weight. Aboveground fresh (AGB_{fresh}) and dry biomass (AGB_{dry}) was obtained by scaling the weight to 1 m^2. Vegetation carbon (C) and nitrogen content (N) of dry samples from Fendt and Rottenbuch collected between 2019 and 2020 were analysed using an elemental analyzer (vario Max cube, Elementar Analysensysteme GmbH, Germany). Species composition was determined only at the Bayreuth sites, where the Shannon-Weaver diversity index was subsequently calculated (Ortiz-Burgos, 2016). A detailed description of the sampling design and sampling can be found in Schucknecht et al. (2020).

2.3. *Statistical analyses*

Spearman's rank correlation and R^2 were used to examine the relationship between *in situ* vegetation traits and predictor variables derived from UAV imagery. Spearman correlation, a non-parametric measure, assessed the strength and direction of monotonic relationships, while R^2 quantified the proportion of variance in vegetation traits explained by the predictor variables (Dodge, 2008). These statistical analyses were conducted across all selected time frames (see Section 2.4.1 below) to account for temporal variations and improve model performance.

2.4. *Regression models*

Classic and automated ML methods were applied to estimate different grassland traits from UAV imagery. The RF (Lange et al., 2025) and Extreme Gradient Boosting (XGBoost; (Chen & Guestrin, 2016)) algorithms are well-known classical machine learning methods for various regression tasks with remote sensing data. RF, a representative of the decision-tree-based 'ensemble learning' approaches, uses bagging (bootstrap aggregation) to enhance model performance and mitigate overfitting. During the bagging process, RF creates an ensemble of decision trees by randomly selecting samples and features from both the in-situ training data and remote sensing predictor variables. This technique enables RF regression to produce robust predictions and provide measurements of variable importance, leveraging multiple decision trees trained on diverse subsets of the data. Similar to RF, XGBoost is also a decision-tree-based ensemble learning method that uses boosting techniques to construct a robust regression model by combining multiple weak learners. It sequentially builds decision trees, where each tree corrects the errors of its predecessors by minimizing a specified loss function using gradient descent. XGBoost also integrates regularization

Table 1
Summary of site characteristics and data collection.

Study area	Sites	Total number of plots	Management	In-situ data	UAV data acquisition dates	
Fendt Rottenbuch	Fendt Rottenbuch	4 2	Intensive: 4–5 cuts and 4–5 slurry applications per year Extensive: 1–2 cut and no slurry	AGB Canopy height C content N content	**2019:** April 24 May 17 June 07 June 25 July 15 Aug 01 Sep 16 Oct 18 **2021:** May **2023:** June 13	**2020:** May 06 June 24 July 27 Oct 01 **2022:** June 01 Aug 02
Bayreuth	Gubitzmoos Obernschreez Schobertsberg	20 for 2022 9 for 2023 5 for 2022 7 for 2023 5 for 2022 6 for 2023	Intensive: 4–5 cuts and 4–5 slurry applications per year	AGB Canopy height Species richness	**2022:** May 16–19 **2023:** April 17–19	

techniques to mitigate overfitting and enhance generalization.

AutoML is an approach designed to automate the process of creating robust ensemble ML models by combining multiple algorithms or statistical models (Baratchi et al., 2024). AutoML utilizes both bagging and boosting techniques to create strong ensemble models. It constructs an optimal ensemble model by combining various algorithms and statistical models such as Linear Regression, Logistic Regression, Decision Trees, RF, and advanced boosting models like LightGBM and XGBoost. The best-fitting model is identified based on its performance metrics. The estimation of vegetation traits in this study was performed using a RF package in R 4.4.2, the Forest-based and Boosted regression model, and AutoML tool in ArcGIS Pro 3.2 software.

Hyperparameter optimization was performed for each time-specific dataset using Random Search (Rebust) with cross-validation for both RF and XGBoost models. For RF, the number of trees was systematically varied between 50 and 500 in increments of 10. Model performance was evaluated at each iteration using the coefficient of determination (R^2), and the best-performing configuration was selected based on the highest R^2 value, which was typically achieved with 250–350 trees. For XGBoost, the number of boosting rounds was varied between 50 and 500, and the optimal configuration was selected similarly based on R^2, typically ranging from 200 to 400 rounds.

2.4.1. Training data subset definition

Two types of training data subsets were created to account for spatial and temporal variability: time-specific training subsets (covering four different time frames) and site-specific training subsets (corresponding to different locations). Four time-specific training subsets were created to train the models, each representing different time frames. This approach aimed to better utilize the available data, enhance model accuracy, and account for the effects of temporal variations on model performance. The time frames were selected based on the available *in situ* data and corresponding vegetation growth stages. The definitions of the time frames are as follows:

- **Entire time series:** Consists of all available *in situ* measurements and UAV data collected throughout the study period.
- **Peak growing season in 2019–2023:** Focuses on *in situ* measurement and UAV data from the peak vegetation growth period in June of each year.
- **Intra-annual data within 2019:** Contains multiple observations within 2019.
- **Single observation data**: Consists of individual observations from all available *in situ* measurements and UAV data.

Six site-specific training subsets were created to train and validate the models, each capturing spatial variability across different locations. This approach enables the assessment of predictive power and the potential of using multi-year data to estimate vegetation traits across different locations. The definitions of the site-specific training subsets are as follows:

- **Fendt multi-year data:** Consists of all available *in situ* measurements and UAV data collected throughout the study period.
- **Fendt single observation data:** Consists of individual observations from all available *in situ* measurements and UAV data.
- **Rottenbuch multi-year data:** Consists of all available *in situ* measurements and UAV data collected throughout the study period.
- **Rottenbuch single observation data:** Consists of individual observations from all available *in situ* measurements and UAV data.
- **Gubitzmoos and Obernschreez single observation data:** Consists of individual observations from all available *in situ* measurements and UAV data.
- **Schobertsberg single observation data:** Consists of individual observations from all available *in situ* measurements and UAV data.

2.4.2. Regression model test cases

To improve estimation accuracy, we conducted test cases by training the regression models using time-specific training subsets of AGB_{dry} and UAV data from the Fendt and Rottenbuch sites. These included entire time series (2019–2023), peak growing season (June 2019–2023), and single observation data (Table A-1 in Supplementary Material). Model test cases were also conducted using site-specific training subsets to determine whether a regression model trained on data from one site could accurately predict AGB_{dry}, species richness, and Shannon H-index at another site when using data collected same time (Table A-1 Test cases 4–5). This approach allowed us to understand how temporal variation in vegetation patterns and the diversity of UAV imagery affected model performance, enabling us to improve predictions under different vegetation and light conditions.

2.4.3. Model assessment

Regression models were evaluated using the coefficient of determination (R^2), regression error, root mean squared error (RMSE), and Mean Absolute Percentage Error (MAPE). These evaluation metrics were calculated from each independent estimate to assess the performance of the regression model in two cases. First, model performance was evaluated by randomly selecting 20 % of the available *in situ* data as an independent validation dataset, while the remaining 80 % were used for training. Second, in cases involving site-specific training subsets, *in situ* measurement and UAV data from one or two sites (Fendt or Gubitzmoos and Obernschreez) were used for training, while *in situ* measurement and UAV data from the other site (Rottentbuch and Schobertsberg) were used for validation (see Table A-1). For AutoML, a set of regression models was evaluated by comparing their RMSE values to determine the best model. The model with the highest R^2 and the lowest RMSE was considered the most accurate and best model in this study. Model performance was assessed using cross-validation.

3. Results

3.1. Field measurements of vegetation traits across study sites

Multi-year vegetation traits data were collected from the Fendt and Rottenbuch sites for the years 2019 to 2023, and from the Bayreuth area for the years 2022–2023. The data consist of AGB_{dry}, canopy height, species richness, and vegetation N and C content. In the total of 36 plots sampled, the values of each vegetation parameter varied depending on the period and site (Fig. 2).

For intra-annual measurements in Fendt and Rottenbuch in 2019, the lowest AGB_{dry} value ranged from 0.5 to 13 g m^{-2} after mowing, while the highest value ranged from 250 to 320 g m^{-2}, measured shortly before grass harvesting. For the canopy height, the lowest values varied between 2.1 to 5.2 cm, while the highest values ranged from 8.5 to 25.8 cm. Regarding chemical parameters derived from AGB samples, N content ranged from 1.2 to 5.9 wt%, and the C content varied between 39.7 and 53.7 wt% (for further details on the comparison between the intensively and extensively managed sites at Rottenbuch, see Figure A-1 in supplementary material).

In 2020, intra-annual measurements in Fendt and Rottenbuch showed the lowest AGB_{dry} values ranging from 0.97 to 9.6 g m^{-2} after mowing, while the highest values varied from 226 to 308 g m^{-2} before harvesting. Canopy height ranged from 2.8 to 7.1 cm at its lowest and 15.3 to 18 cm at its highest. Chemical parameters derived from AGB samples indicated N content ranging from 1.4 to 4.5 wt%, and the C content from 39.7 to 46.8 wt%.

For inter-annual measurements during the peak growing season at all sites, significant differences were found for AGB_{dry} and canopy height between 2020 and 2023. For instance, the lowest AGB_{dry} values ranged from 0.52 to 8.5 g m^{-2} after mowing, while the highest values ranged from 35.3 to 251.2 g m^{-2}. Canopy height ranged from 4.2 to 6 cm at its lowest and 16.8 to 18.9 cm at its highest. At Bayreuth sites, species

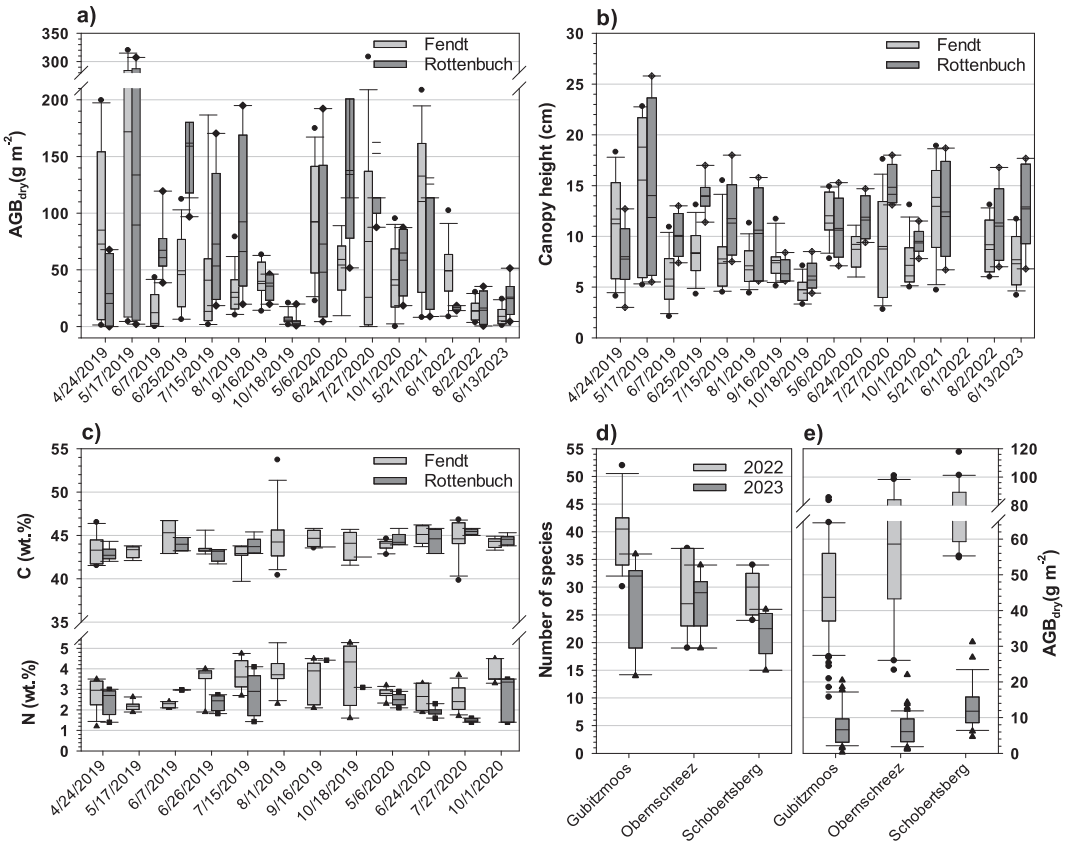

Fig. 2. Multi-year vegetation traits data collection and variation at Fendt and Rottenbuch (a–c), and study sites around Bayreuth (d–e) in 2019–2023.

richness ranged from 19 to 52 in May 2022 and compared to 14–36 in April 2023. Similarly, AGB_{dry} values ranged from 15.7 to 117.5 g m^{-2} in May 2022, but declined from 0.3 to 31.2 g m^{-2} in April 2023.

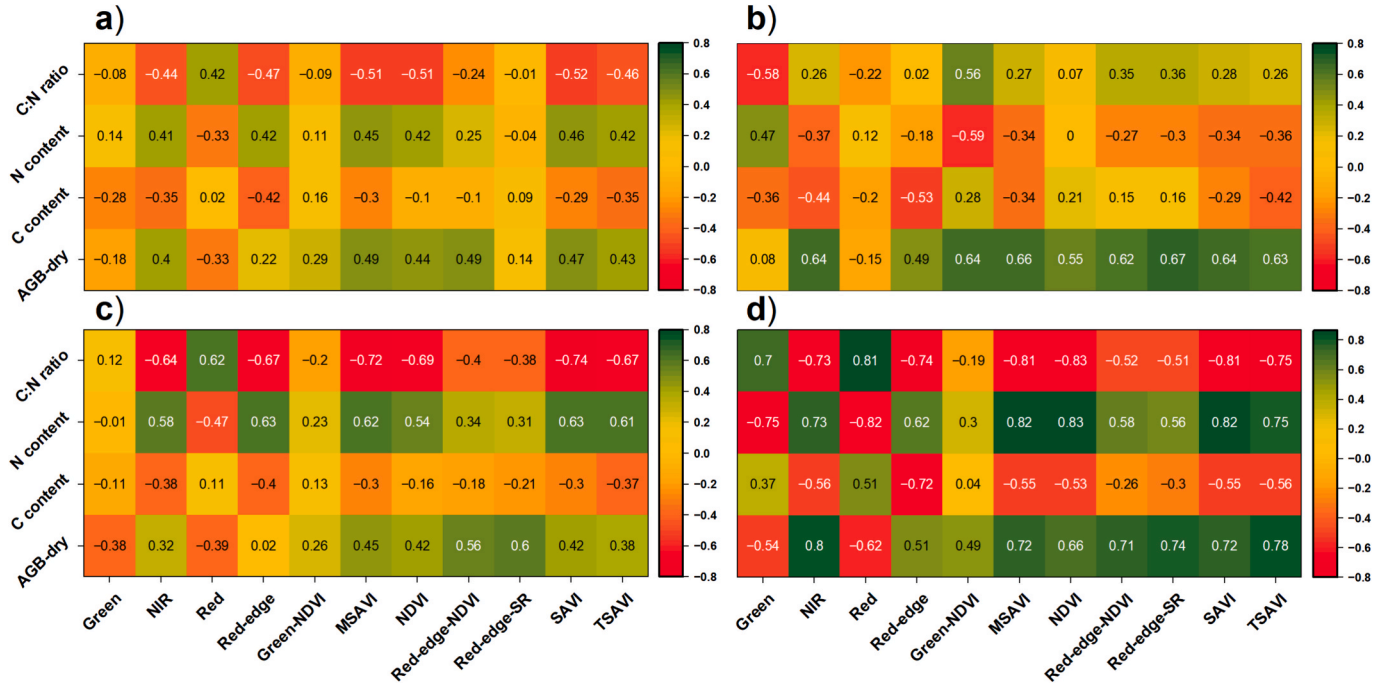

Fig. 3. Matrix illustrating the relationship between UAV-based predictor variables and vegetation traits across different time frames: a) Correlation for the entire time series (2019–2023), b) Correlation for peak growing seasons (June 2019–2023), c) Correlation for intra-annual data within 2019, and d) Correlation for a single observation data (April 24, 2019).

3.2. Estimating vegetation traits using regression models

3.2.1. Relationship between UAV-based predictor variables and vegetation traits

The correlation coefficient and R^2 value were calculated between eleven predictor variables extracted from the UAV imagery and vegetation traits across the four different time frames defined in the previous Section 2.4.1. The predictor variables that showed strong correlations with vegetation traits varied across different growth periods (Fig. 3).

Overall, most spectral bands and VIs had a medium to high correlation with AGB_{dry}, ranging between 0.6 and 0.8 ($R^2 = 0.4–0.63$ and $p < 0.02$). Among them, the NIR band, red-edge band, and all VIs had the strongest correlations with AGB_{dry} ($p < 0.01$). However, correlation coefficients varied depending on the selected time frame. In terms of periods, higher positive correlation coefficients between AGB_{dry} and predictor variables were observed when using the peak growing season (June 2019–2023) and the single observation data (April 24, 2019 and $p < 0.01$) (Fig. 3-b, d). Specifically, AGB_{dry} showed strong correlations with NIR band, MSAVI, NDVI, SAVI and TSAVI when using single observation data (Fig. 3-d and $p < 0.01$)).

Focusing on chemical parameters, C content showed a weak positive correlation with $NDVI_{green}$, NDVI, $NDVI_{red\text{-}edge}$ and $SR_{red\text{-}edge}$ when using data from the peak growing season (June 2019–2023) and intra-annual data within 2019 ($p < 0.05$). However, some of these indices were negatively correlated with C content in other periods. On the contrary, N content showed medium to strong positive correlations with the NIR band, red-edge band, MSAVI, NDVI, SAVI, and TSAVI when using the entire time series data (2019–2023, and $p < 0.01$), intra-annual data within 2019 and for a single observation data. In particular, the strongest positive correlations were detected when using the single observation data (Fig. 3-d). C:N ratio showed medium to high positive correlations with the red band, and $NDVI_{green}$ when using data from the intra-annual data within 2019 and the single observation data ($p < 0.05$).

The primary reason for these variations was significant changes in illumination conditions. Fig. 4 presents a violin graph illustrating how illumination conditions varied considerably from 2019 to 2020 across the study sites. A comparison of solar irradiance values of the red, green, NIR, and red-edge bands at Fendt and Rottenbuch shows that irradiance at Fendt was consistently lower than at Rottenbuch from April 24 to June 25, 2019. However, between July 15 and September 16 in 2019, the values at both sites became closer. From October 18, 2019 to July 27, 2020, Fendt again exhibited lower irradiance values. These fluctuations in lighting conditions affected spectral reflectance and could lead to inconsistencies in the relationship between predictor variables and vegetation traits. Furthermore, we compared the relationship between R^2 values for AGB_{dry} estimation, which used intra-annual data within 2019, and irradiance differences across all spectral bands at the Fendt and Rottnbuch sites (for further details on the comparison, see figure A-11 in supplementary material). In this comparison, the irradiance differences were calculated as the difference between the average irradiance values of each band at the Fendt and Rottnbuch sites. The comparison result showed a moderate negative correlation between R^2 values and irradiance differences, ranging from −0.41 to −0.46. This suggests that lower irradiance differences between Fendt and Rottnbuch are associated with higher R_2 values for AGB_{dry} estimation. Overall, the results suggest that the most suitable time frames for training ML models are the peak growing season (June 2019–2023) and the single observation data, as these periods may provide reasonably accurate estimates.

3.2.2. Regression model test cases used to predict vegetation traits

The model performed with low accuracy, achieving R-squared values of 0.31–0.42 when using entire time series and 0.54 when using peak growing season data, demonstrating that it is not reliable in predicting AGB_{dry} across different temporal conditions (Table A-1 in supplementary material). UAV imagery was captured under varying conditions of cloud cover, sun angle, surface moisture, and lighting throughout the study period. These inconsistencies were a primary factor contributing to the reduced accuracy of the regression models in estimating AGB_{dry} when using entire datasets or long-term data. This finding is consistent with the results of the correlation analysis in the previous section. On the contrary, regression models using single observations achieved medium to high accuracy with R-squared values of 0.55–0.89, suggesting its reliability in predicting vegetation traits in the entire time series for monitoring.

Furthermore, we trained regression models using single observation data of Fendt, and Gubitzmoos and Obernschreez separately, and then applied these site-specific trained models to predict AGB_{dry} in Rottenbuch and AGB_{dry}, species richness, and Shannon index in the Schobertsberg site, which were not part of the training dataset. The results indicate that the regression models performed poorly at Fendt ($R^2 = 0.15–0.21$) but performed well at Schobertsberg ($R^2 = 0.61–0.71$). These findings suggest that if UAV images are taken under relatively similar conditions, it may be possible to use a regression model trained on data from one site to accurately predict vegetation traits at another site.

Overall, the test case analysis suggested that using single observations achieved medium to high accuracy. Therefore, we selected single

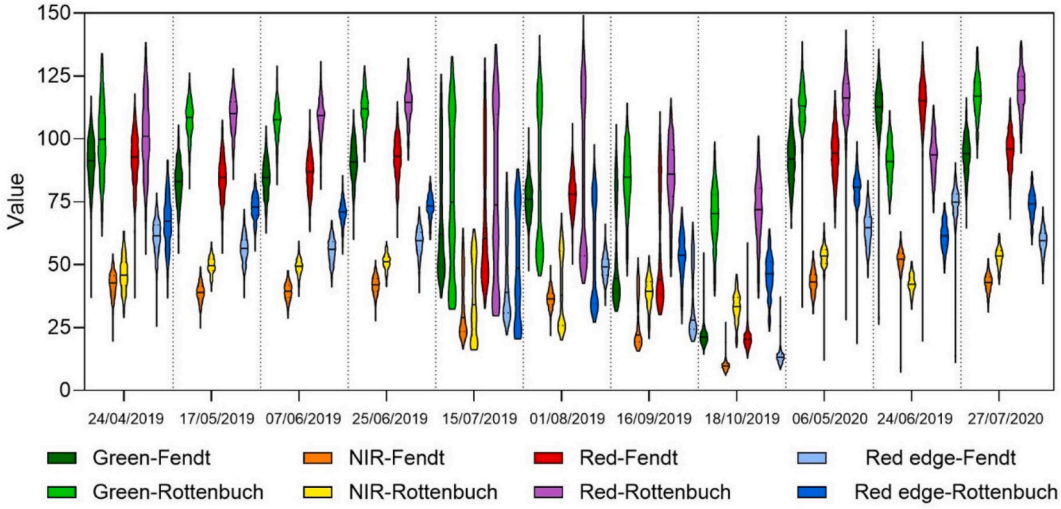

Fig. 4. Solar irradiance measured by sunshine sensor in 2019–2020.

observation data as the best model for spatial mapping, which is presented in the next section.

3.2.3. Spatial mapping of vegetation traits

Using regression models applied separately to single observations in 2019–2023, we estimated the spatial distribution and intra- and inter-annual variations of vegetation traits at the site scale in intensively and extensively managed grasslands. The validation results show that the average R-squared value was 0.81 for $AGB_{dry,}$ 0.77 for N content, 0.81 for C:N ratio, 0.84 for species richness, and 0.86 for Shannon index, respectively (Fig. 5-a). The average RMSE was 29.5 for AGB_{dry}, 0.4 for N content, 1.7 for C:N ratio, 7 for species richness, and 0.4 for Shannon index, respectively (Fig. 5-b). The average MAPE was 1.2 for AGB_{dry}, 0.5 for N content, 0.4 for C:N ratio, 0.2 for species richness, and 0.3 for Shannon index, respectively.

Using the regression models in an upscaling approach can produce detailed spatial and temporal distributions of vegetation traits across the study sites. For example, for the sites in the TERENO pre-Alpine observatory in Fendt and Rottenbuch, Figs. 6 and 7 shows selected parcels illustrating the spatial distribution of the estimated vegetation traits on July 15, 2019.

The spatial distribution of the estimated AGB_{dry}, N content, and C:N ratio exhibited clear patterns influenced by mowing practices and site-specific grassland management. AGB_{dry} varied significantly across the sites, highlighting differences e.g. in landscape, soil, and plant development stages after respective mowing events. N content and the C:N ratio provided valuable insights into plant nutrient status, with noticeable variation across different sites.

For the sites in Bayreuth, AGB_{dry}, Shannon H-index, and species richness were estimated separately for 2022 and 2023. Fig. 8 shows an example of the estimated vegetation traits at Obernschreez from May 16 to 19, 2022. Additionally, Figure A-5 in the Supplementary material provides details on the estimated vegetation traits for April 17–19, 2023, along with a comparison of these traits between 2022 and 2023.

The obtained maps showed variations in AGB_{dry} and plant diversity, emphasizing differences in biodiversity across sites. Similarly, AGB_{dry}, Shannon index, and Species richness demonstrated clear spatial patterns and varied by site-specific management. These results demonstrate the effectiveness of the regression models in capturing fine-scale spatial and temporal variations in vegetation traits, which could support ecological monitoring and sustainable management decisions.

3.3. Comparison of temporal changes in plant traits at parcels

As each plot is managed site-specifically, the mowing events were not the same for all plots. As a result, a multi-year comparison of plots was not appropriate. Instead, we conducted an intra-annual comparative analysis based on changes in mowing events.

A mowing-event-based comparative analysis was performed between selected grassland parcels from April to October 2019. Event-based percentage changes in AGB_{dry} are presented in the Ribbon chart (Fig. 9), while spatiotemporal changes in AGB_{dry} are illustrated in the maps below (Fig. 10). Focusing on intensively managed grassland parcels at Fendt, AGB_{dry} was generally high before the first mowing event. For instance, at FE2, AGB_{dry} ranged from 25 to 150 g m^{-2} on April 24, 2019, and increased to 150–300 g m^{-2} by May 17, 2019. However, AGB_{dry} decreased sharply to 0–25 g m^{-2} after the first mowing. After the first mowing, AGB_{dry} started growing back, reaching up to 150 g m^{-2} before the second mowing event, but the regrowth was highly variable across the parcel. AGB_{dry} was mostly in the range of 25–50 g m^{-2} and 50–75 g m^{-2} between the first and second mowing. After the second mowing event, AGB_{dry} regrowth was in the range of 25–50 g m^{-2}. The third mowing event took place on October 18, 2019.

For the extensively managed RB2 parcel, AGB_{dry} was as low as 25 g m^{-2} at the beginning of the growing season (April 24–May 17, 2019) and increased to 50–75 g m^{-2} across most of the parcel by June 07, 2019 (Fig. 9-b). At peak growth (June 25, 2019), AGB_{dry} reached 150–200 g m^{-2} in 11 % of the parcel, 100–150 g m^{-2} in 41 %, 75–100 g m^{-2} in 19 %, and 50–75 g m^{-2} in 28 %, respectively. The results highlight the progressive increase in AGB_{dry} throughout the growing season, though the growth pattern varied across the parcel (Fig. 10). However, half of the parcel was mowed by July 15, 2019, resulting in a sharp decline in AGB_{dry} in some areas. Following the first mowing, AGB_{dry} began to recover, though the growth pattern varied across the parcel with a final mowing on September 16, 2019.

Overall, AGB_{dry} values were typically low in field measurements conducted immediately after hay making or in parcels that were frequently cut, whereas higher AGB_{dry} values were observed when measurements were taken just before mowing events. In some cases, the comparison clearly showed that while one parcel was mowed, another parcels had not yet been mowed, or that some parcels were partially or incompletely mowed.

For chemical contents, the comparison of N content and C:N ratio between paired parcels showed distinct spatial and temporal patterns influenced by management practices and environmental conditions (Figs. 11 and 12). Before the first mowing, N content in FE1 varied, with 35 % of the parcel ranging from 2 to 2.5 wt%, 43 % from 2.5 to 3 wt%, and 20 % from 3 to 3.5 wt%. For FE2, N content was mostly 1.5–2 wt% in 13 % of the parcel, 2–2.5 wt% in 38 %, and 2.5–3 wt% in 44 %. During the first and second mowing periods, N content in FE1 fell to 0.5–2 wt% immediately after mowing, while it later increased to 3–4.5 wt% as the vegetation regrew in both parcels. The rise in N content is possibly due to fertilization and the presence of young vegetation. After the final mowing event, N content was initially dominated by 3–3.5 wt% in most

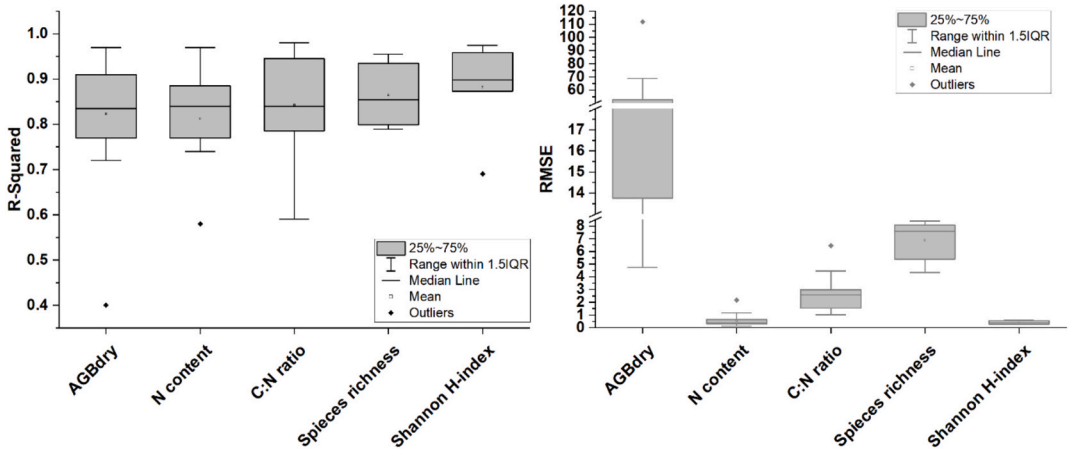

Fig. 5. Regression models performance boxplot, showing the distribution of metrics across all observations.

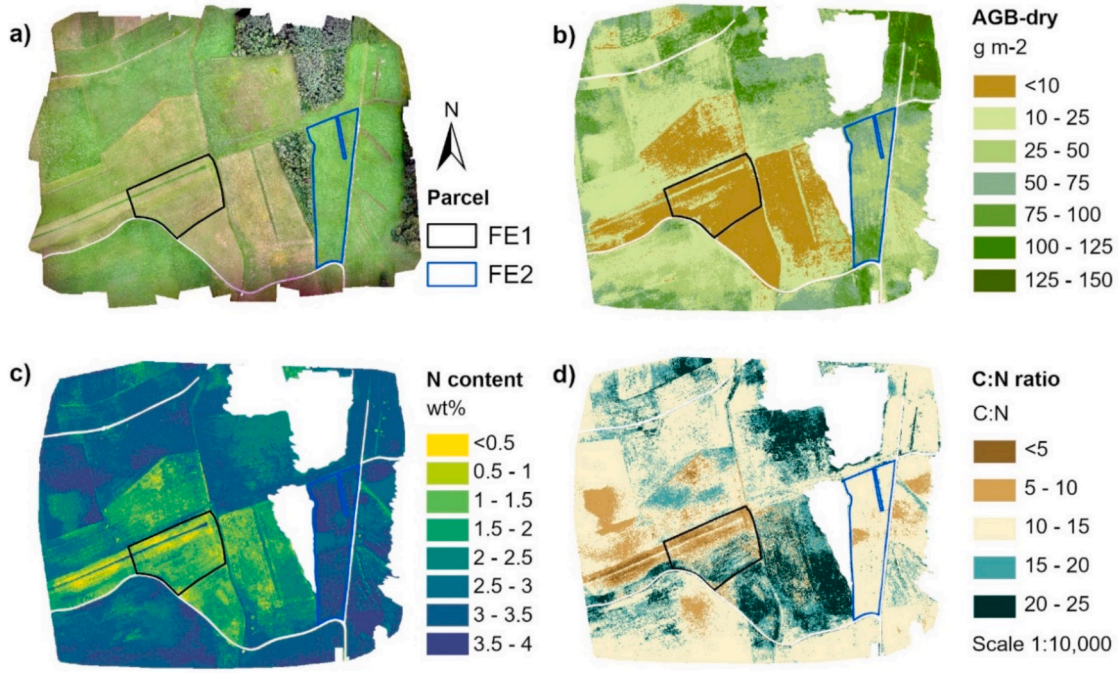

Fig. 6. Estimated vegetation traits at Fendt on July 15, 2019. Here, the maps show aerial view of the grassland parcels in Fendt (a), the estimated AGB_{dry} (b), N content (c), and C:N ratio (d).

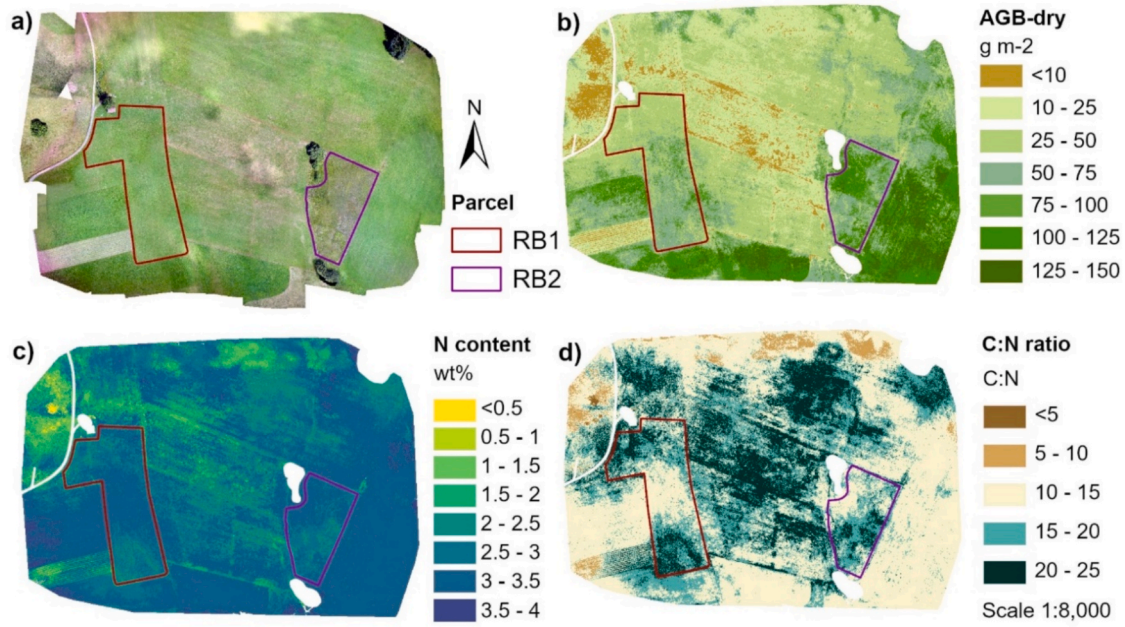

Fig. 7. Estimated vegetation traits at Rottenbuch on July 15, 2019. Here, the maps show aerial view of the grassland parcels in Rottenbuch (a), the estimated AGB_{dry} (b), N content (c), and C:N ratio (d).

parts of both parcels. For extensively managed RB2 parcel, N content was below 0.5 wt% in 14 % of the parcel, 1.5–2 wt% in 58 %, and 2–2.5 wt% in 18 % before the first mowing event. During the peak growing period, the dominant N content increased to 2–3.5 wt%, occupying 85 % of the parcel on 15 July 2019, while 3.5–4 wt% covered 84 % of the parcel on 1 August 2019. After the first mowing, the dominant N content decreased to 0.5–1 wt%, covering 50 % of the parcel, while 1–1.5 wt%, 1.5–2 wt%, and 2–2.5 wt% each separately covered 15 % of the parcel. At the end of the growing season, N content of 1.5–2 wt% covered most of the parcel. Overall, comparison results showed that seasonal changes in N content differed between intensively and extensively managed parcels. In intensively managed parcels, the dominant N content value started at a moderate level in spring, peaked at 2–3.5 wt% during the growing season, and then dropped sharply to 0.5–1 wt% after mowing, followed by a gradual recovery. In contrast, extensively managed parcels had a more stable N content, starting low in spring, peaking at lower values during the growing season, rising after the first mowing, and gradually decreasing to a low level in autumn due to less frequent cutting and fertilization.

Generally, the C:N ratio showed significant differences between

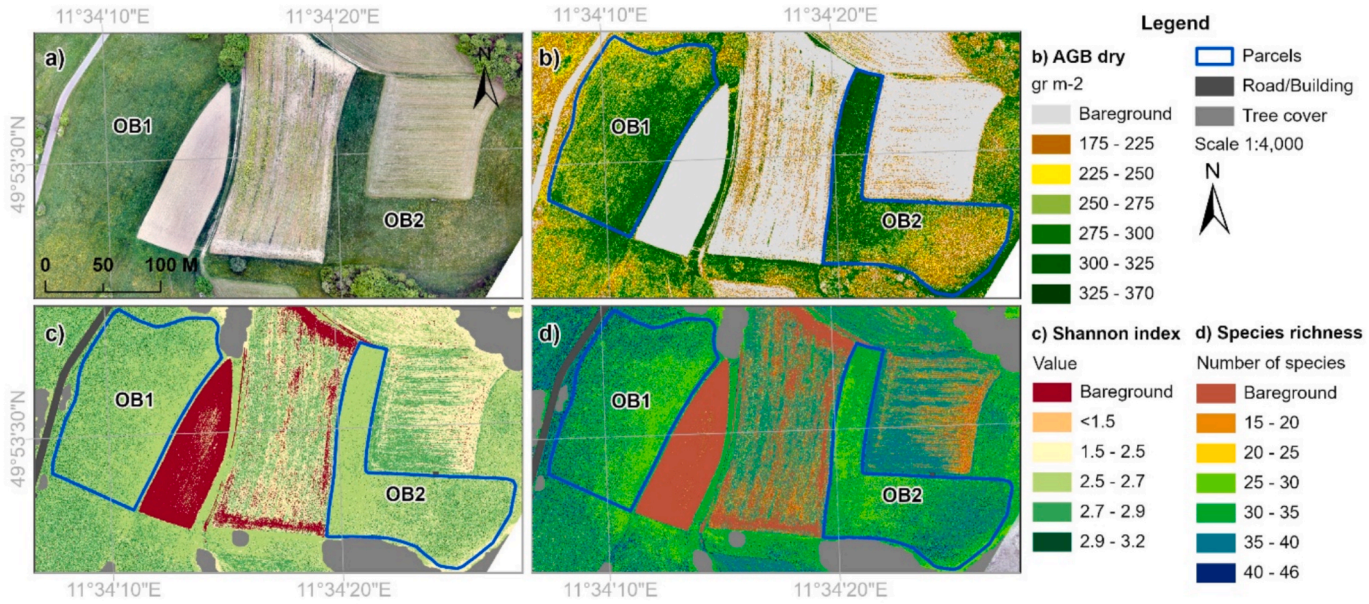

Fig. 8. The estimated vegetation traits of Obernschreez in Bayreuth. Here, the maps show aerial view of the grassland parcels (a), the estimated AGB_{dry} (b), Shannon H-index (c), and Species richness (d) from May 16 to 19, 2022.

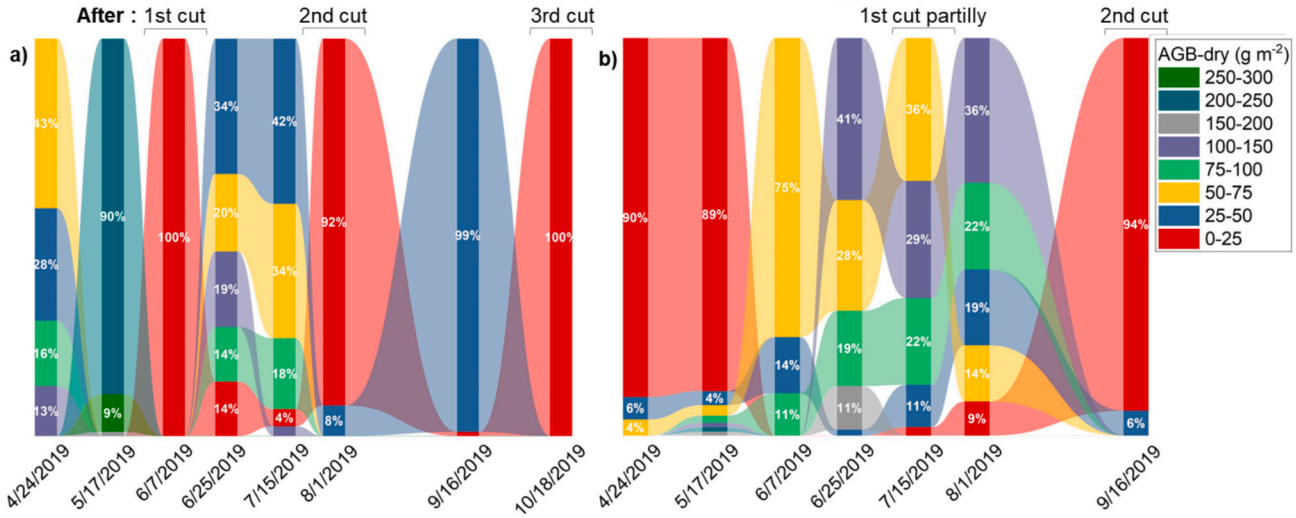

Fig. 9. Event-based percentage changes in AGB_{dry} in 2019: a) FE2 parcel and b) RB2 parcel.

paired parcels with different management practices (Fig. 12). For instance, moderate C:N ratios (10–20) were observed in all intensively managed parcels in 24 April 2019. After the first mowing event, lower (<10) and moderate C:N ratios increased in FE1 and FE2, while higher C:N ratios (20–30) increased in RB1. Observations of low to moderate C:N ratios during the peak of the growing months indicate seasonal changes in plant growth, nutrient uptake, and organic matter decomposition. Furthermore, moderate C:N ratios remained dominant after the second mowing, while a mix of moderate to high C:N ratios dominated in autumn. For the extensively managed RB2 parcel, higher C:N ratios were observed in spring, while moderate to high C:N ratios were pronounced during the peak growing months. After the first mowing, C:N ratios remained stable at moderate levels, while high and strongly high (30–35) C:N ratios emerged in autumn. These increases in C:N ratios indicated slower decomposition and delayed nutrient release.

We also conducted a comparative analysis at selected pair parcels (OB1 and OB2) in Obernschreez, as shown in Fig. 8 above and Fig. A-10 in Supplementary Material. Results showed that the mean AGB_{dry} value was 280.21 g m^{-2} in OB1 and 270.01 g m^{-2} in OB2 before mowing in May 2022 and 36 g m^{-2} in OB1 and 30.83 g m^{-2} in OB2 in April 2023. The average number of species was 32 in OB1 and 33 in OB2 in May 2022, and 26 in OB1 and 25 in OB2 in April 2023. The mean value of the Shannon H-index was 2.66 in OB1 and 2.6 in OB2 in May 2022, and 2.15 in OB1 and 2.02 in OB2 in April 2023, respectively. Overall, the AGB_{dry}, H-index, and the number of species were higher in May 2022 and lower in April 2023 at both pair parcels, likely due to variations in mowing events, plant growth stages, and environmental conditions.

4. Discussion

4.1. Estimating vegetation traits from multi-year drone images

To estimate vegetation traits, we aimed to combine the advantages of the long-term collected *in situ* data and UAV imagery with ML. Previous work in the study region indicated that the lack of high-quality field data for training can be a challenge for estimating vegetation traits from UAV

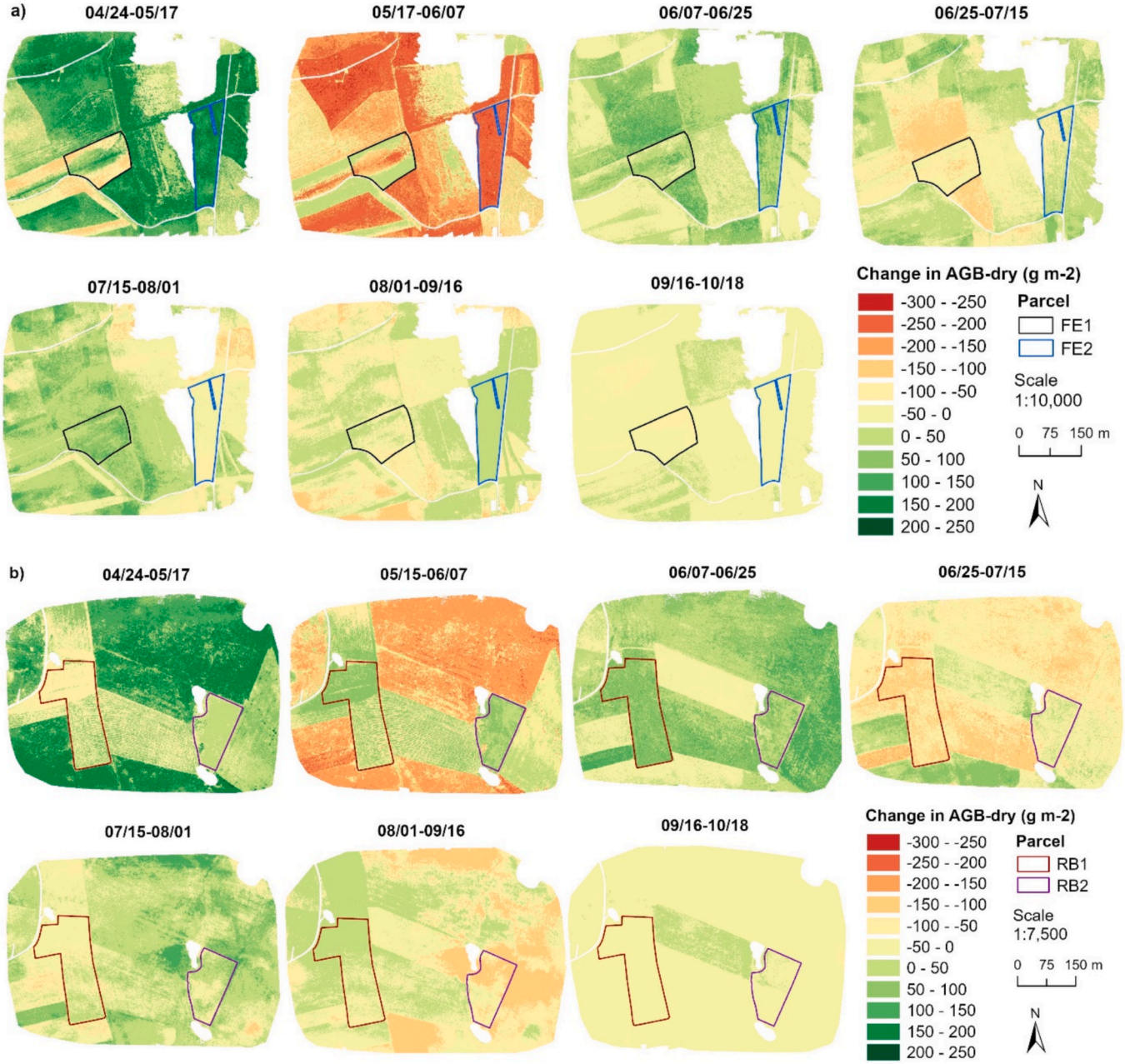

Fig. 10. The comparison of AGB_{dry} at different parcels in 2019: a) Change in AGB_{dry} in Fendt and b) Change in AGB_{dry} in Rottenbuch.

imagery, especially N content (Schucknecht et al., 2022). For this reason, we collected long-term high-quality *in situ* data along with corresponding UAV imagery, which provides critical information for understanding changes and dynamics in vegetation traits. When utilizing these multi-year data, we considered how well the *in situ* data correlated with the predictor variables derived from the UAV imagery, which spectral variables could contribute the most significantly, and which regression models were best suited for estimating different vegetation traits.

Therefore, we firstly identified the most potential spectral variables based on our previous work and a literature review (Dashpurev et al., 2023; Schucknecht et al., 2022; Thornley et al., 2023; Zhang et al., 2024). In our study, the relationships between vegetation traits and variables such as NIR band, red-edge band, NDVI, $NDVI_{red\text{-}edge}$, and MSAVI were relatively strong and positive, although depending on the selected time period. These observations align with previous similar studies. For instance, numerous recent studies have demonstrated that the spectral bands and vegetation indices as mentioned above are effective for estimating AGB_{dry}, (Bazzo et al., 2023a; Lussem et al., 2019; Pan et al., 2024), N content and C:N ratio (Dal Lago et al., 2024) and species diversity (Bazzo et al., 2024; Lyu et al., 2024).

Subsequently, we selected regression models based on our previous comparative analyses and the AutoML technique to identify the most suitable options. AutoML is a powerful tool for evaluating different regression models and determining their suitability for estimating vegetation traits, such as AGB (Alvarez-Mendoza et al., 2022) and grass height (César de Sá et al., 2022). AutoML simplifies the process of identifying optimal algorithms without the need for extensive manual effort by automating processes such as model selection, hyperparameter tuning, and performance evaluation. In this study, AutoML was used to compare seven regression models and the results showed that RF and XGBoost performed the best when applied to single-date observation data. Many studies have demonstrated the effectiveness of RF and XGBoost in estimating vegetation traits from remotely sensed data.

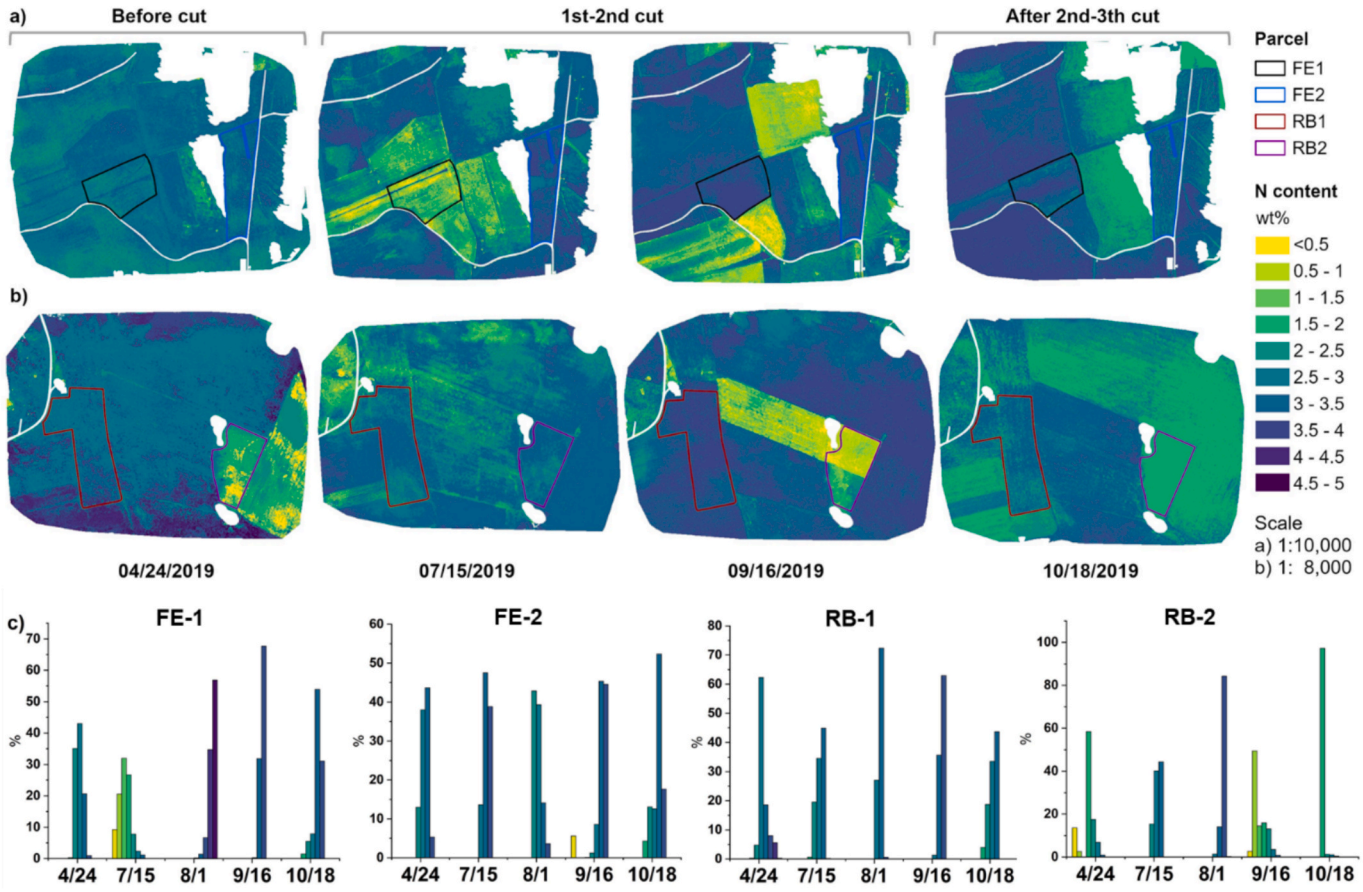

Fig. 11. The comparison of N content at different parcels in 2019. Here, the maps show the estimated N content in Fendt (a) and Rottenbuch (b). The bar graph (c) shows the percentage of N content classes per parcel.

These algorithms are widely recognized for their reasonable accuracy, especially in predicting AGB, N content and biodiversity etc., (Arogoundade et al., 2023; Lyu et al., 2024; Yang et al., 2024; Zhang et al., 2024), making them valuable tools for remote sensing in vegetation studies.

Furthermore, our vegetation traits dataset covers multiple years, and we initially hypothesized that this extensive dataset could improve the accuracy and reliability of vegetation trait estimates. However, the multi-year images were captured under varying conditions, such as differences in illumination, cloud cover, sun angles, and ground moisture. These factors made it challenging to integrate the multi-year data into a single training dataset for regression models. This integration process faces a typical radiometric inconsistency effect (Jenerowicz et al., 2023; Zhu et al., 2024). Several radiometric calibration methods have been developed for multispectral UAV imagery; however, they still have their disadvantages and limitations, and there is no universal method to solve this issue completely (Daniels et al., 2023; Guo et al., 2019). In Fig. 4, the violin graph shows that illumination conditions varied significantly over time between the Fendt and Rottenbuch study sites. UAV imagery at Fendt was mostly captured in the morning, while images at the Rottenbuch were taken in the afternoon. Additionally, the intra-annual data was collected from spring to autumn, leading to seasonal variations in observation angle, illumination condition, and sun angle throughout the multi-year UAV imagery. It can be seen from Fig. 4 that solar irradiance values for each band at Rottenbuch are mostly higher than those at Fendt over the entire observation period. Consequently, the spectral predictor variables derived from UAV imagery are affected by radiometric inconsistencies. For instance, a recent assessment of different radiometric calibration methods highlighted the impact of variations in reflectance and vegetation indices on the estimation of AGB (Zhu et al., 2024). Despite radiometric calibration, temporal inconsistencies often persist in UAV imagery. For example, Olsson et al. (2021) recently assessed the accuracy of the Parrot Sequoia camera and its sunshine sensor for radiometric correction of multispectral UAV images. Their findings indicated that factors such as camera temperature and atmospheric conditions significantly affected radiometric accuracy, suggesting that even with calibration, temporal inconsistencies can remain. Therefore, our study suggests collecting UAV imagery under consistent lighting conditions or at the same time of day utilizing standardized methods for future monitoring purposes.

The radiometric inconsistencies posed challenges for integrating long-term data into a single regression model, however, we achieved relatively accurate estimates of vegetation traits by training separate regression models using the time-specific training subset data (a single observation date). After radiometric calibration, several strategies are commonly employed to further reduce residual inconsistencies in multi-year imagery. Time-specific modeling is one such post-calibration approach aimed at reducing the effects of radiometric variability. In particular, the results showed that the regression models performed well with R-squared values of 0.81 for AGB_{dry}, 0.77 for N content, 0.81 for C:N ratio, 0.88 for Shannon H-index, and 0.86 for species richness. These findings are comparable to those reported by Bazzo et al. (Bazzo et al., 2023b) for AGB, Xu et al. (Xu et al., 2023) for N content and C:N ratio, and Bazzo et al. (Bazzo et al., 2024) for species richness.

4.2. *Monitoring changes in vegetation traits using estimated data*

The main usage of estimation is to monitor changes in vegetation traits due to management and provide high-resolution spatio-temporal information to farmers and decision-makers. Our result demonstrated

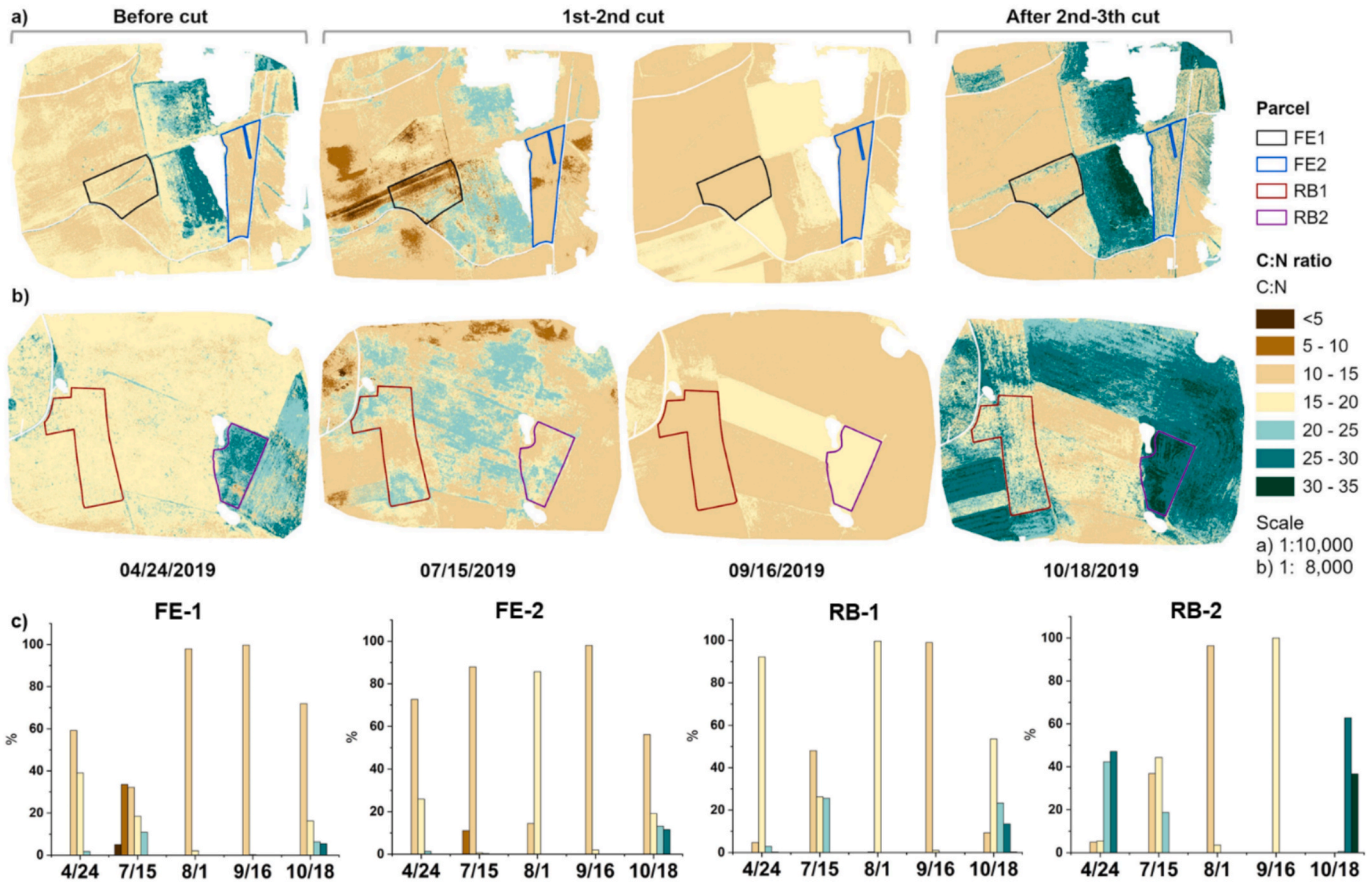

Fig. 12. The comparison of C:N ratio at paired parcels in 2019. Here, the maps show the estimated C:N ratio in Fendt (a) and Rottenbuch (b). The bar graph (c) shows the percentage of C:N ratio classes per parcel.

that spatio-temporal maps of vegetation traits can be effectively obtained by combining multi-year *in-situ* data with UAV imagery. Monitoring vegetation traits across intra- and inter-annual timescales is essential for sustainable grassland management and understanding how ecosystems respond to environmental changes and management activities. However, inter-annual comparisons were ineffective in our case because each parcel is managed site-specifically, and mowing events were not consistent across all parcels. Additionally, mowing events varied in terms of time within each parcel. For example, when considering changes in AGB_{dry} at FE1 in June 2019–2023, FE1 was partially mowed on 25 June 2019, whereas it was completely mowed on 24 June 2020. Furthermore, the FE1 parcel was not mowed on 01 June 2022 but was mowed on 13 June 2023. Therefore, one of the limitations of this study is that our multi-year data is not continuous, making it unsuitable for multi-year comparisons. However, it remains useful for intra-annual analysis based on mowing events.

For intra-annual spatio-temporal analysis, intra-annual variations in vegetation traits showed distinct patterns influenced by seasonal changes and differences in management intensity (Figs. 9–12). For AGB_{dry}, frequently cut areas showed higher AGB values, ranging from 250 to 350 g m^{-2}, while the extensively managed plot (RB2) displayed higher values, ranging from 200 to 260 g m^{-2} during the vegetation growing season (April to October 2019). In intensively managed sites, AGB was significantly lower right after mowing events but showed rapid regrowth throughout the growing months due to improved growth conditions and regular fertilization throughout the year (Botter et al., 2021). According to Petersen et al. (2021) the annual biomass production decreased continuously with the frequency of mowing events. For fertilization, manure events are typically scheduled before the growing season or the first mowing, and again after the first and third mowing events (Petersen et al., 2021). In contrast, extensively managed grasslands displayed slower AGB accumulation throughout the growing season due to minimal or no fertilization.

Seasonal dynamics of vegetation N content in managed grasslands vary due to management practices, plant species composition, and environmental conditions (Wang & Schjoerring, 2012). Our study demonstrated that seasonal patterns in N content were also evident, with intensively managed sites showing higher N values, particularly during the growing season (Fig. 11). Conversely, extensively managed sites experienced lower and more consistent N content across the growing season. This temporal variation in N cycling is likely influenced by fertilization-mowing cycles, as previous studies have highlighted that intensive management significantly increases vegetation N content compared to extensive management (Zistl-Schlingmann et al., 2020). Furthermore, a study conducted in pre-alpine managed grasslands showed that N content in AGB_{dry} was highest in late spring or early summer, decreased during the growing months, and remained moderate in autumn (Schlingmann et al., 2020). Our intra-annual estimates also showed moderate to high N content within the parcels following mowing events. This could be related to the presence of young vegetation that emerges after mowing, as young plants typically have higher N content due to their need for nitrogen accumulation to support rapid growth and development (Thion et al., 2016). Additionally, the moderate to high N content estimates could be associated with intensive management practices, which tend to provide higher N content in AGB throughout the season due to the frequent mowing of younger biomass (Reyes et al., 2015).

The C:N ratio highlighted differences in nutrient dynamics. In intensively managed sites, C:N ratios remained low and stable due to rapid nutrient turnover from mowing and fertilization. Furthermore,

seasonal variations in C:N ratios at intensively managed parcels demonstrated low to moderate ratios in late spring and the growing months, and moderate to high ratios in autumn. These seasonal dynamics are influenced by intensive management practices, which result in increased nitrogen availability that accelerates decomposition during the early growing months and slows it down in autumn (Gill et al., 2022). In contrast, extensively managed sites showed higher C:N ratios, especially in late summer and early autumn, indicating slower decomposition rates and reduced nitrogen availability. Overall, the mowing event-based intra-annual changes in AGB_{dry}, N content, and C:N ratio demonstrate how intensive and extensive management differently influences vegetation dynamics throughout the growing season in temperate grasslands.

Species richness and the Shannon H-index are important indicators for monitoring the effects of grassland management. These variables are influenced by grassland management practices, growth stages, and climate conditions (Corentin Babin et al., 2023; Manning et al., 2015; Weisser et al., 2017). According to Maria (2018), the mean species richness of grassland in 11 plots (100 m^2) at the Bayreuth study area was 32.27 (± .37) in the growing season. Our study shows species richness ranging from 19 to 52 (avg. 35.8) in May 16–19 2022, and from 14 to 36 (avg. 26.1) in April 17–19, 2023. Comparing the two years, species richness was higher in 2022 than in 2023 (Fig. 2-d). This difference can be attributed to the sampling occurring one month earlier in 2022 compared to 2023. Additionally, frequent fertilization and mowing events may have contributed to the decrease in species richness from 2022 to 2023.

5. Conclusion

This study showed the estimation of vegetation traits by integrating *in situ* data with multi-year UAV imagery using ML regression models. The *in situ* vegetation traits data consisted of ABG_{dry}, C content, N content, C:N ratio and species diversity in pre-Alpine managed grasslands. In the estimation context, correlation analysis was conducted between vegetation traits and eleven predictor variables extracted from UAV imagery across different time frames. The correlation results suggested that the peak growing season or single observation data are the most suitable time frames for training ML regression models, rather than using the entire time series.

We further selected regression models based on previous expertise and AutoML, which allowed for a systematic comparison of models and identified the most suitable approaches for our data. The accuracy of vegetation trait estimates depended heavily on the chosen algorithm and selected period of time, as the multi-year images were captured under varying illumination conditions, leading to spectral inconsistency. Consequently, future research should prioritize collecting UAV imagery under consistent lighting conditions or at the same time of day, using standardized methods.

However, the spatial distribution of vegetation traits was separately estimated with acceptable accuracy by using single observation datasets or by combining data captured under similar lighting conditions. ML can effectively address minor spectral inconsistencies by modeling complex nonlinear relationships between spectral predictor variables and vegetation traits. Additionally, incorporating vegetation indices (NDVI, MSAVI, etc.,) that are less sensitive to spectral inconsistencies can enhance model robustness and estimation accuracy, especially when analyzing multi-year data.

The multidimensional dataset was created from the final vegetation traits map products, allowing us to assess event-based spatiotemporal changes across several selected grassland parcels. This spatiotemporal comparative analysis demonstrated an effective approach for monitoring intra-annual variations in vegetation traits, and the results will be used as input for further modeling. The results of spatiotemporal analysis are particularly essential for understanding the impacts of management intensification on grassland ecosystem functions and sustainable management.

CRediT authorship contribution statement

Batnyambuu Dashpurev: Writing – original draft, Visualization, Methodology, Investigation, Formal analysis, Data curation, Conceptualization. **David R. Piatka:** Writing – review & editing, Methodology, Investigation, Data curation. **Alexander Krämer:** Writing – original draft, Resources, Methodology, Investigation, Funding acquisition, Data curation, Conceptualization. **Anne Schucknecht:** Writing – review & editing, Methodology, Investigation, Data curation, Conceptualization. **Klaus Butterbach-Bahl:** Writing – review & editing, Supervision, Conceptualization. **Ralf Kiese:** Writing – review & editing, Supervision, Resources, Methodology, Funding acquisition, Conceptualization.

Funding

This work was funded by the German Federal Ministry of Education and Research (BMBF) in the SUSALPS project (Sustainable use of alpine and prealpine grassland soils in a changing climate, funding number 031B0516A) and the CarboGrass project (Impact of grassland management on soil carbon storage, funding number 031B1396).

Declaration of competing interest

The authors declare the following financial interests/personal relationships which may be considered as potential competing interests: Batnyambuu Dashpurev reports financial support, article publishing charges, equipment, drugs, or supplies, statistical analysis, and travel were provided by Karlsruhe Institute of Technology. Batnyambuu Dashpurev reports a relationship with Karlsruhe Institute of Technology that includes: employment. If there are other authors, they declare that they have no known competing financial interests or personal relationships that could have appeared to influence the work reported in this paper.

Acknowledgments

We are grateful to our colleagues from KIT for their valuable support during the field and laboratory work. Their contributions were essential to the successful completion of this study.

Appendix A. Supplementary data

Supplementary data to this article can be found online at https://doi.org/10.1016/j.ecolind.2025.114371.

Data availability

Data will be made available on request.

References

Alvarez-Mendoza, C.I., Guzman, D., Casas, J., Bastidas, M., Polanco, J., Valencia-Ortiz, M., Montenegro, F., Arango, J., Ishitani, M., Selvaraj, M.G., 2022. Predictive modeling of above-ground biomass in *Brachiaria pastures* from satellite and UAV imagery using machine learning approaches. Remote Sens. 14 (22), 5870. https://doi.org/10.3390/RS14225870.

Arogoundade, A.M., Mutanga, O., Odindi, J., Naicker, R., 2023. The role of remote sensing in tropical grassland nutrient estimation: a review. Environ. Monitor. Assess. 195 (8), 1–20. https://doi.org/10.1007/S10661-023-11562-6.

Baratchi, M., Wang, C., Limmer, S., van Rijn, J.N., Hoos, H., Bäck, T., Olhofer, M., 2024. Automated machine learning: past, present and future. Artif. Intell. Rev. 57 (5), 1–88. https://doi.org/10.1007/S10462-024-10726-1.

Bardgett, R.D., Bullock, J.M., Lavorel, S., Manning, P., Schaffner, U., Ostle, N., Chomel, M., Durigan, G., Fry, L.E., Johnson, D., Lavallee, J.M., Le Provost, G., Luo, S., Png, K., Sankaran, M., Hou, X., Zhou, H., Ma, L., Ren, W., Shi, H., 2021. Combatting global grassland degradation. Nat. Rev. Earth Environ. 2 (10), 720–735. https://doi.org/10.1038/s43017-021-00207-2.

Bazzo, C.O.G., Kamali, B., dos Santos Vianna, M., Behrend, D., Hueging, H., Schleip, I., Mosebach, P., Haub, A., Behrendt, A., Gaiser, T., 2024. Integration of UAV-sensed features using machine learning methods to assess species richness in wet grassland ecosystems. Eco. Inform. 83, 102813. https://doi.org/10.1016/J.ECOINF.2024.102813.

Bazzo, C.O.G., Kamali, B., Hütt, C., Bareth, G., Gaiser, T., 2023a. A review of estimation methods for aboveground biomass in grasslands using UAV. Remote Sens. 15 (3), 639. https://doi.org/10.3390/RS15030639.

Bazzo, C.O.G., Kamali, B., Hütt, C., Bareth, G., Gaiser, T., 2023b. A review of estimation methods for aboveground biomass in grasslands using UAV. Remote Sens. 15 (3), 639. https://doi.org/10.3390/RS15030639.

Bengtsson, J., Bullock, J.M., Egoh, B., Everson, C., Everson, T., O'Connor, T., O'Farrell, P. J., Smith, H.G., Lindborg, R., 2019. Grasslands—more important for ecosystem services than you might think. Ecosphere 10 (2), e02582. https://doi.org/10.1002/ECS2.2582.

Berauer, B.J., Wilfahrt, P.A., Reu, B., Schuchardt, M.A., Garcia-Franco, N., Zistl-Schlingmann, M., Dannenmann, M., Kiese, R., Kühnel, A., Jentsch, A., 2020. Predicting forage quality of species-rich pasture grasslands using vis-NIRS to reveal effects of management intensity and climate change. Agric. Ecosyst. Environ. 296, 106929. https://doi.org/10.1016/J.AGEE.2020.106929.

Berger, K., Verrelst, J., Féret, J.B., Wang, Z., Wocher, M., Strathmann, M., Danner, M., Mauser, W., Hank, T., 2020. Crop nitrogen monitoring: recent progress and principal developments in the context of imaging spectroscopy missions. Remote Sens. Environ. 242, 111758. https://doi.org/10.1016/J.RSE.2020.111758.

Biswal, S., Pathak, N., Chatterjee, C., Mailapalli, D.R., 2024. Estimation of aboveground biomass from spectral and textural characteristics of paddy crop using UAV-multispectral images and machine learning techniques. Geocarto Int. 39 (1). https://doi.org/10.1080/10106049.2024.2364725.

Bobbink, R., Christin, L., Hilde, T. (2022). *Review and revision of empirical critical loads of nitrogen for Europe*.

Botter, M., Zeeman, M., Burlando, P., Fatichi, S., 2021. Impacts of fertilization on grassland productivity and water quality across the European Alps under current and warming climate: Insights from a mechanistic model. Biogeosciences 18 (6), 1917–1939. https://doi.org/10.5194/BG-18-1917-2021.

Bronson, K.F., Conley, M.M., French, A.N., Hunsaker, D.J., Thorp, K.R., Barnes, E.M., 2020. Which active optical sensor vegetation index is best for nitrogen assessment in irrigated cotton? Agron. J. 112 (3), 2205–2218. https://doi.org/10.1002/AGJ2.20120.

César de Sá, N., Baratchi, M., Buitenhuis, V., Cornelissen, P., van Bodegom, P.M., 2022. AutoML for estimating grass height from ETM+/OLI data from field measurements at a nature reserve. Gisci. Remote Sens. 59 (1), 2164–2183. https://doi.org/10.1080/15481603.2022.2152304.

Chen, T., Guestrin, C., 2016. XGBoost: a Scalable tree boosting system. In: *Proceedings of the ACM SIGKDD International Conference on Knowledge Discovery and Data Mining*. https://doi.org/10.1145/2939672.2939785.

Corentin Babin, Sandrine Espagnol, Joël Aubin. (2023). Effects of agricultural practices on biodiversity. A review. In *HAL*. https://hal.science/hal-04465927v1.

Dal Lago, P., Vavlas, N., Kooistra, L., De Deyn, G.B., 2024. Estimation of nitrogen uptake, biomass, and nitrogen concentration, in cover crop monocultures and mixtures from optical UAV images. Smart Agric. Technol. 9, 100608. https://doi.org/10.1016/J.ATECH.2024.100608.

Daniels, L., Eeckhout, E., Wieme, J., Dejaegher, Y., Audenaert, K., Maes, W.H., 2023. Identifying the optimal radiometric calibration method for UAV-based multispectral imaging. Remote Sens 15 (11), 2909. https://doi.org/10.3390/RS15112909.

Dashpurev, B., Dorj, M., Phan, T.N., Bendix, J., Lehnert, L.W., 2023. Estimating fractional vegetation cover and aboveground biomass for land degradation assessment in eastern Mongolia steppe: combining ground vegetation data and remote sensing. Int. J. Remote Sens. 44 (2), 452–468. https://doi.org/10.1080/01431161.2023.2165421.

Dodge, Y., 2008. Spearman rank correlation coefficient. Concise Encycl. Stat. 502–505. https://doi.org/10.1007/978-0-387-32833-1_379.

Dumont, B., Andueza, D., Niderkorn, V., Lüscher, A., Porqueddu, C., Picon-Cochard, C., 2015. A meta-analysis of climate change effects on forage quality in grasslands: specificities of mountain and Mediterranean areas. Grass Forage Sci. 70 (2), 239–254. https://doi.org/10.1111/GFS.12169.

Ennaji, O., Vergütz, L., El Allali, A., 2023. Machine learning in nutrient management: a review. Artif. Intell. Agric. 9, 1–11. https://doi.org/10.1016/J.AIIA.2023.06.001.

Fauvel, M., Lopes, M., Dubo, T., Rivers-Moore, J., Frison, P.L., Gross, N., Ouin, A., 2020. Prediction of plant diversity in grasslands using Sentinel-1 and -2 satellite image time series. Remote Sens. Environ. 237, 111536. https://doi.org/10.1016/J.RSE.2019.111536.

Feigenwinter, I., Hörtnagl, L., Zeeman, M.J., Eugster, W., Fuchs, K., Merbold, L., Buchmann, N., 2023. Large inter-annual variation in carbon sink strength of a permanent grassland over 16 years: impacts of management practices and climate. Agric. For. Meteorol. 340, 109613. https://doi.org/10.1016/J.AGRFORMET.2023.109613.

Fumy, F., Schwarz, C., Fartmann, T., 2023. Intensity of grassland management and landscape heterogeneity determine species richness of insects in fragmented hay meadows. Global Ecol. Conserv. 47, e02672. https://doi.org/10.1016/J.GECCO.2023.E02672.

Furnitto, N., Ramírez-Cuesta, J.M., Intrigliolo, D.S., Todde, G., Failla, S., 2025. Remote sensing for pasture biomass quantity and quality assessment: challenges and future prospects. Smart Agric. Technol. 12, 101057. https://doi.org/10.1016/J.ATECH.2025.101057.

Gao, J., Han, M., Zhang, D., Ma, Z., Zhang, Y., Fu, S., Liang, T., 2025. Cross-scale estimating of forage nitrogen in alpine grassland integrating UAV imagery and Sentinel-2 data. Eur. J. Agron. 170, 127760. https://doi.org/10.1016/J.EJA.2025.127760.

Gao, J., Liang, T., Liu, J., Yin, J., Ge, J., Hou, M., Feng, Q., Wu, C., Xie, H., 2020. Potential of hyperspectral data and machine learning algorithms to estimate the forage carbon-nitrogen ratio in an alpine grassland ecosystem of the Tibetan Plateau. ISPRS J. Photogramm. Remote Sens. 163, 362–374. https://doi.org/10.1016/J.ISPRSJPRS.2020.03.017.

Gilhaus, K., Boch, S., Fischer, M., Hölzel, N., Kleinebecker, T., Prati, D., Rupprecht, D., Schmitt, B., Klaus, V.H., 2017. Grassland management in Germany: Effects on plant diversity and vegetation composition. Tuexenia 37 (1), 379–397. https://doi.org/10.14471/2017.37.010.

Gill, A.L., Adler, P.B., Borer, E.T., Buyarski, C.R., Cleland, E.E., D'Antonio, C.M., Davies, K.F., Gruner, D.S., Harpole, W.S., Hofmockel, K.S., MacDougall, A.S., McCulley, R.L., Melbourne, B.A., Moore, J.L., Morgan, J.W., Risch, A.C., Schütz, M., Seabloom, E.W., Wright, J.P., Hobbie, S.E., 2022. Nitrogen increases early-stage and slows late-stage decomposition across diverse grasslands. J. Ecol. 110 (6), 1376–1389. https://doi.org/10.1111/1365-2745.13878.

Gomez-Casanovas, N., Blanc-Betes, E., Moore, C.E., Bernacchi, C.J., Kantola, I., DeLucia, E.H., 2021. A review of transformative strategies for climate mitigation by grasslands. Sci. Total Environ. 799, 149466. https://doi.org/10.1016/J.SCITOTENV.2021.149466.

Guo, Y., Senthilnath, J., Wu, W., Zhang, X., Zeng, Z., Huang, H., 2019. Radiometric calibration for multispectral camera of different imaging conditions mounted on a UAV platform. Sustainability 11 (4), 978. https://doi.org/10.3390/SU11040978.

He, X., Zhao, K., Chu, X., 2021. AutoML: a survey of the state-of-the-art. Knowl.-Based Syst. 212, 106622. https://doi.org/10.1016/j.knosys.2020.106622.

Hörtnagl, L., Barthel, M., Buchmann, N., Eugster, W., Butterbach-Bahl, K., Díaz-Pinés, E., Zeeman, M., Klumpp, K., Kiese, R., Bahn, M., Hammerle, A., Lu, H., Ladreiter-Knauss, T., Burri, S., Merbold, L., 2018. Greenhouse gas fluxes over managed grasslands in Central Europe. Glob. Chang. Biol. 24 (5), 1843–1872. https://doi.org/10.1111/GCB.14079.

Huang, S., Tang, L., Hupy, J.P., Wang, Y., Shao, G., 2021. A commentary review on the use of normalized difference vegetation index (NDVI) in the era of popular remote sensing. J. For. Res. 32 (1), 1–6. https://doi.org/10.1007/S11676-020-01155-1/FIGURES/2.

Janga, B., Asamani, G.P., Sun, Z., Cristea, N., 2023. A Review of practical AI for remote sensing in earth sciences. Remote Sens. 15 (16), 4112. https://doi.org/10.3390/RS15164112.

Jenerowicz, A., Wierzbicki, D., Kedzierski, M., 2023. Radiometric correction with topography influence of multispectral imagery obtained from unmanned aerial vehicles. Remote Sens. 15 (8), 2059. https://doi.org/10.3390/RS15082059.

Kameyama, S., Sugiura, K., 2021. Effects of differences in structure from motion software on image processing of unmanned aerial vehicle photography and estimation of crown area and tree height in forests. Remote Sens. 13 (4), 626. https://doi.org/10.3390/RS13040626.

Kiese, R., Fersch, B., Baessler, C., Brosy, C., Butterbach-Bahl, K., Chwala, C., Dannenmann, M., Fu, J., Gasche, R., Grote, R., Jahn, C., Klatt, J., Kunstmann, H., Mauder, M., Rödiger, T., Smiatek, G., Soltani, M., Steinbrecher, R., Völksch, I., Kiese, C., 2018. The TERENO pre-alpine observatory: integrating meteorological, hydrological, and biogeochemical measurements and modeling. Vadose Zone J. 17 (1), 1–17. https://doi.org/10.2136/VZJ2018.03.0060.

Kirschke, D., Häger, A., Schmid, J.C., 2021. New Trends and Drivers for Agricultural Land Use in Germany. Springer, Cham, pp. 39–61.

Korell, L., Andrzejak, M., Berger, S., Durka, W., Haider, S., Hensen, I., Herion, Y., Höfner, J., Kindermann, L., Klotz, S., Knight, T.M., Linstädter, A., Madaj, A.M., Merbach, I., Michalski, S., Plos, C., Roscher, C., Schädler, M., Welk, E., Auge, H., 2024. Land use modulates resistance of grasslands against future climate and inter-annual climate variability in a large field experiment. Glob. Chang. Biol. 30 (7), e17418. https://doi.org/10.1111/GCB.17418.

Kupidura, P., Kępa, A., Krawczyk, P., 2024. Comparative analysis of the performance of selected machine learning algorithms depending on the size of the training sample. Rep. Geodesy Geoinf. 118 (1), 53–69. https://doi.org/10.2478/RGG-2024-0015.

Lange, T.M., Gültas, M., Schmitt, A.O., Heinrich, F., 2025. optRF: Optimising random forest stability by determining the optimal number of trees. BMC Bioinf. 26 (1), 1–21. https://doi.org/10.1186/S12859-025-06097-1/FIGURES/5.

Lemenkova, P., 2025. Machine learning algorithms of remote sensing data processing for mapping changes in land cover types over central apennines. Italy. J. Imaging 11 (5), 153. https://doi.org/10.3390/JIMAGING11050153.

Li, C., Peng, F., Xue, X., You, Q., Lai, C., Zhang, W., Cheng, Y., 2018. Productivity and quality of alpine grassland vary with soil water availability under experimental warming. Front. Plant Sci. 871, 398944. https://doi.org/10.3389/FPLS.2018.01790/BIBTEX.

Lussem, U., Bolten, A., Menne, J., Gnyp, M.L., Schellberg, J., Bareth, G. (2019). Estimating biomass in temperate grassland with high resolution canopy surface models from UAV-based RGB images and vegetation indices. *Https://Doi.Org/10.1117/1.JRS.13.034525*, *13*(3), 034525. https://doi.org/10.1117/1.JRS.13.034525.

Lyu, X., Li, X., Dang, D., Wang, K., Zhang, C., Cao, W., Lou, A., 2024. Systematic review of remote sensing technology for grassland biodiversity monitoring: current status and challenges. Global Ecol. Conserv. 54, e03196. https://doi.org/10.1016/J.GECCO.2024.E03196.

Manning, P., Gossner, M.M., Bossdorf, O., Allan, E., Zhang, Y.Y., Prati, D., Blüthgen, N., Boch, S., Böhm, S., Börschig, C., Hölzel, N., Jung, K., Klaus, V.H., Klein, A.M., Kleinebecker, T., Krauss, J., Lange, M., Müller, J., PAŠALIĆ, E., Fischer, M., 2015. Grassland management intensification weakens the associations among the

diversities of multiple plant and animal taxa. Ecology 96 (6), 1492–1501. https://doi.org/10.1890/14-1307.1.
Maria Dittmann. (2018). *Species Richness in an Urban Landscape - Scale Dependence of Phytodiversity* [Master Thesis, University of Bayreuth]. https://www.researchgate.net/publication/338336801_Species_Richness_in_an_Urban_Landscape_-_Scale_Dependence_of_Phytodiversity.
Mayel, S., Jarrah, M., Kuka, K., 2021. How does grassland management affect physical and biochemical properties of temperate grassland soils? A review study. Grass Forage Sci. 76 (2), 215–244. https://doi.org/10.1111/GFS.12512.
Montero, D., Aybar, C., Mahecha, M.D., Martinuzzi, F., Söchting, M., Wieneke, S., 2023. A standardized catalogue of spectral indices to advance the use of remote sensing in earth system research. Sci. Data 10 (1), 1–20. https://doi.org/10.1038/s41597-023-02096-0.
Morais, T.G., Teixeira, R.F.M., Figueiredo, M., Domingos, T., 2021. The use of machine learning methods to estimate aboveground biomass of grasslands: a review. Ecol. Ind. 130, 108081. https://doi.org/10.1016/J.ECOLIND.2021.108081.
Schmitt, M.T., Haensel, M., Kaim, A., Lee, H., Reinermann, S., Koellner, T., 2024. Recreation and its synergies and trade-offs with other ecosystem services of Alpine and pre-Alpine grasslands. Regional Environ. Change 24 (2), 1–16. https://doi.org/10.1007/S10113-024-02213-8/FIGURES/5.
Norasma, C.Y.N., Fadzilah, M.A., Roslin, N.A., Zanariah, Z.W.N., Tarmidi, Z., Candra, F. S., 2019. Unmanned aerial vehicle applications in agriculture. IOP Conf. Ser.: Mater. Sci. Eng. 506 (1), 012063. https://doi.org/10.1088/1757-899X/506/1/012063.
Offermanns, L., Tiemeyer, B., Dettmann, U., Rüffer, J., Düvel, D., Vogel, I., Brümmer, C., 2023. High greenhouse gas emissions after grassland renewal on bog peat soil. Agric. For. Meteorol. 331, 109309. https://doi.org/10.1016/J.AGRFORMET.2023.109309.
Olsson, P.O., Vivekar, A., Adler, K., Garcia Millan, V.E., Koc, A., Alamrani, M., Eklundh, L., 2021. Radiometric correction of multispectral UAS images: evaluating the accuracy of the parrot sequoia camera and sunshine sensor. Remote Sens. 13 (4), 577. https://doi.org/10.3390/RS13040577.
Ortiz-Burgos, S., 2016. Shannon-weaver diversity index. Encycl. Earth Sci. Ser. 572–573. https://doi.org/10.1007/978-94-017-8801-4_233.
Pan, T., Ye, H., Zhang, X., Liao, X., Wang, D., Bayin, D., Safarov, M., Okhonniyozov, M., Majid, G., 2024. Estimating aboveground biomass of grassland in central Asia mountainous areas using unmanned aerial vehicle vegetation indices and image textures – a case study of typical grassland in Tajikistan. Environ. Sustain. Indic. 22, 100345. https://doi.org/10.1016/J.INDIC.2024.100345.
Peerbhay, K., Adelabu, S., Lottering, R., Singh, L., 2022. Mapping carbon content in a mountainous grassland using SPOT 5 multispectral imagery and semi-automated machine learning ensemble methods. Sci. Afr. 17, e01344. https://doi.org/10.1016/J.SCIAF.2022.E01344.
Petersen, K., Kraus, D., Calanca, P., Semenov, M.A., Butterbach-Bahl, K., Kiese, R., 2021. Dynamic simulation of management events for assessing impacts of climate change on pre-alpine grassland productivity. Eur. J. Agron. 128, 126306. https://doi.org/10.1016/J.EJA.2021.126306.
Raj, R., Kar, S., Nandan, R., Jagarlapudi, A., 2019. Precision agriculture and unmanned aerial vehicles (UAVs). Unmanned Aerial Veh. 7–23. https://doi.org/10.1007/978-3-030-27157-2_2/FIGURES/2.
Reyes, J., Schellberg, J., Siebert, S., Elsaesser, M., Adam, J., Ewert, F., 2015. Improved estimation of nitrogen uptake in grasslands using the nitrogen dilution curve. Agron. Sustain. Dev. 35 (4), 1561–1570. https://doi.org/10.1007/S13593-015-0321-2/FIGURES/4.
Salehin, I., Islam, M.S., Saha, P., Noman, S.M., Tuni, A., Hasan, M.M., Baten, M.A., 2024. AutoML: a systematic review on automated machine learning with neural architecture search. J. Inf. Intell. 2 (1), 52–81. https://doi.org/10.1016/J.JIIXD.2023.10.002.
Schlingmann, M., Tobler, U., Berauer, B., Garcia-Franco, N., Wilfahrt, P., Wiesmeier, M., Jentsch, A., Wolf, B., Kiese, R., Dannenmann, M., 2020. Intensive slurry management and climate change promote nitrogen mining from organic matter-rich montane grassland soils. Plant Soil 456 (1–2), 81–98. https://doi.org/10.1007/S11104-020-04697-9/TABLES/6.
Schmitt, T.M., Riebl, R., Martín-López, B., Hänsel, M., Koellner, T., 2022. Plural valuation in space: mapping values of grasslands and their ecosystem services. Ecosyst. People 18 (1), 258–274. https://doi.org/10.1080/26395916.2022.2065361.
Schoof, N., Luick, R., Jürgens, K., Jones, G., 2020. Dairies in Germany: key factors for grassland conservation? Sustainability 12 (10), 4139. https://doi.org/10.3390/SU12104139.
Schucknecht, A., Krämer, A., Asam, S., Mejia-Aguilar, A., Garcia-Franco, N., Schuchardt, M.A., Jentsch, A., Kiese, R., 2020. Vegetation traits of pre-alpine grasslands in southern Germany. Sci. Data 7 (1), 1–11. https://doi.org/10.1038/s41597-020-00651-7.
Schucknecht, A., Seo, B., Krämer, A., Asam, S., Atzberger, C., Kiese, R., 2022. Estimating dry biomass and plant nitrogen concentration in pre-Alpine grasslands with low-cost UAS-borne multispectral data-a comparison of sensors, algorithms, and predictor sets. Biogeosciences 19 (10), 2699–2727. https://doi.org/10.5194/BG-19-2699-2022.
Schwarz, C., Trautner, J., Fartmann, T., 2018. Common pastures are important refuges for a declining passerine bird in a pre-alpine agricultural landscape. J. Ornithol. 159 (4), 945–954. https://doi.org/10.1007/S10336-018-1561-0/TABLES/4.
Seeger, M., 2023. Agricultural soil degradation in Germany. Handb Environ. Chem. 121, 87–103. https://doi.org/10.1007/698_2022_948/FIGURES/4.
Stadler, J., Klotz, S., Brandl, R., Knapp, S., 2017. Species richness and phylogenetic structure in plant communities: 20 years of succession. Web Ecol. 17 (2), 37–46. https://doi.org/10.5194/WE-17-37-2017.
Thion, C.E., Poirel, J.D., Cornulier, T., De Vries, F.T., Bardgett, R.D., Prosser, J.I., 2016. Plant nitrogen-use strategy as a driver of rhizosphere archaeal and bacterial ammonia oxidiser abundance. FEMS Microbiol. Ecol. 92 (7), 91. https://doi.org/10.1093/FEMSEC/FIW091.
Thornley, R.H., Gerard, F.F., White, K., Verhoef, A., 2023. Prediction of grassland biodiversity using measures of spectral variance: a meta-analytical review. Remote Sens. (Basel) 15 (3), 668. https://doi.org/10.3390/RS15030668/S1.
UNESCO World Heritage Centre. (2015). Alpine and pre-alpine meadow and marsh landscapes (historic anthropogenic landscapes in the area of "Werdenfelser Land", "Ammergau", "Staffelseegebiet" and "Murnauer Moos", district Garmisch-Partenkirchen). https://whc.unesco.org/en/tentativelists/5974/.
Verrelst, J., Malenovský, Z., Van der Tol, C., Camps-Valls, G., Gastellu-Etchegorry, J.P., Lewis, P., North, P., Moreno, J., 2019. Quantifying vegetation biophysical variables from imaging spectroscopy data: a review on retrieval methods. Surveys Geophys. 40 (3), 589–629. https://doi.org/10.1007/S10712-018-9478-Y/FIGURES/9.
Vidican, R., Mălinaș, A., Ranta, O., Moldovan, C., Marian, O., Ghețe, A., Ghișe, C.R., Popovici, F., Cătunescu, G.M., 2023. Using remote sensing vegetation indices for the discrimination and monitoring of agricultural crops: a critical review. Agronomy 13 (12), 3040. https://doi.org/10.3390/AGRONOMY13123040/S1.
Vogt, J., Klaus, V.H., Both, S., Fürstenau, C., Gockel, S., Gossner, M.M., Heinze, J., Hemp, A., Hölzel, N., Jung, K., Kleinebecke, T., Lauterbach, R., Lorenzen, K., Ostrowski, A., Otto, N., Prati, D., Renner, S., Schumacher, U., Seibold, S., Weisser, W. W., 2019. Eleven years' data of grassland management in Germany. Biodivers. Data J. 7, e36387. https://doi.org/10.3897/BDJ.7.E36387.
Walsh, O.S., Shafian, S., Marshall, J.M., Jackson, C., McClintick-Chess, J.R., Blanscet, S. M., Swoboda, K., Thompson, C., Belmont, K.M., Walsh, W.L., Walsh, O.S., Shafian, S., Marshall, J.M., Jackson, C., McClintick-Chess, J.R., Blanscet, S.M., Swoboda, K., Thompson, C., Belmont, K.M., Walsh, W.L., 2018. Assessment of UAV based vegetation indices for nitrogen concentration estimation in spring wheat. Adv. Remote Sens. 7 (2), 71–90. https://doi.org/10.4236/ARS.2018.72006.
Wang, L., Schjoerring, J.K., 2012. Seasonal variation in nitrogen pools and 15N/13C natural abundances in different tissues of grassland plants. Biogeosciences 9 (5), 1583–1595. https://doi.org/10.5194/BG-9-1583-2012.
Wang, Y., Qin, R., Cheng, H., Liang, T., Zhang, K., Chai, N., Gao, J., Feng, Q., Hou, M., Liu, J., Liu, C., Zhang, W., Fang, Y., Huang, J., Zhang, F., 2022. Can machine learning algorithms successfully predict grassland aboveground biomass? Remote Sens. (Basel) 14 (16), 3843. https://doi.org/10.3390/RS14163843/S1.
Weisser, W.W., Roscher, C., Meyer, S.T., Ebeling, A., Luo, G., Allan, E., Beßler, H., Barnard, R.L., Buchmann, N., Buscot, F., Engels, C., Fischer, C., Fischer, M., Gessler, A., Gleixner, G., Halle, S., Hildebrandt, A., Hillebrand, H., de Kroon, H., Eisenhauer, N., 2017. Biodiversity effects on ecosystem functioning in a 15-year grassland experiment: patterns, mechanisms, and open questions. Basic Appl. Ecol. 23, 1–73. https://doi.org/10.1016/J.BAAE.2017.06.002.
Xue, J., Su, B., 2017. Significant remote sensing vegetation indices: a review of developments and applications. J. Sens. https://doi.org/10.1155/2017/1353691.
Xu, S., Xu, X., Zhu, Q., Meng, Y., Yang, G., Feng, H., Yang, M., Zhu, Q., Xue, H., Wang, B., 2023. Monitoring leaf nitrogen content in rice based on information fusion of multi-sensor imagery from UAV. Precis. Agric. 24 (6), 2327–2349. https://doi.org/10.1007/S11119-023-10042-8/FIGURES/10.
Yang, Y., Dong, J., Tang, J., Zhao, J., Lei, S., Zhang, S., Chen, F., 2024. Mapping foliar C, N, and P concentrations in an ecological restoration area with mixed plant communities based on LiDAR and hyperspectral data. Remote Sens. 16 (9), 1624. https://doi.org/10.3390/RS16091624.
Zhang, J., Hu, Y., Li, F., Fue, K.G., Yu, K., 2024. Meta-analysis assessing potential of drone remote sensing in estimating plant traits related to nitrogen use efficiency. Remote Sens. (Basel) 16 (5), 838. https://doi.org/10.3390/RS16050838/S1.
Zhao, Y., Liu, Z., Wu, J., 2020. Grassland ecosystem services: a systematic review of research advances and future directions. Landsc. Ecol. 35 (4), 793–814. https://doi.org/10.1007/S10980-020-00980-3/METRICS.
Zhao, Y., Yin, X., Fu, Y., Yue, T., 2022. A comparative mapping of plant species diversity using ensemble learning algorithms combined with high accuracy surface modeling. Environ. Sci. Pollut. Res. 29 (12), 17878–17891. https://doi.org/10.1007/S11356-021-16973-X/FIGURES/6.
Zhu, H., Huang, Y., An, Z., Zhang, H., Han, Y., Zhao, Z., Li, F., Zhang, C., Hou, C., 2024. Assessing radiometric calibration methods for multispectral UAV imagery and the influence of illumination, flight altitude and flight time on reflectance, vegetation index and inversion of winter wheat AGB and LAI. Comput. Electron. Agric. 219, 108821. https://doi.org/10.1016/J.COMPAG.2024.108821.
Zistl-Schlingmann, M., Kengdo, S.K., Kiese, R., Dannenmann, M., 2020. Management intensity controls nitrogen-use-efficiency and flows in grasslands—a 15N tracing experiment. Agronomy 10 (4), 606. https://doi.org/10.3390/AGRONOMY10040606.